Calculations executed for the 2-bladed rotor of the VIRYA-3.9 windmill and the 3-bladed rotor of the VIRYA-3.9B3 windmill (both λ_d = 6, stainless steel tapered blades) driving the VIRYA-4.2 PM-generator for 26 V delta and 26 V star

ing. A. Kragten

July 2022
reviewed January 2025

KD 733

It is allowed to copy this report for private use. A prototype of the VIRYA-3.9 or the VIRYA-3.9B3 wind turbine has not yet been built and tested. No responsibility is accepted for the use of these wind turbines.

Engineering office Kragten Design
Populierenlaan 51
5492 SG Sint-Oedenrode
The Netherlands
telephone: +31 413 475770
e-mail: info@kdwindturbines.nl
website: www.kdwindturbines.nl

Contains page

1 Introduction

Already in June 1978 I have performed measurements on a 2-bladed windmill rotor with tapered blades cut from a cylinder. The rotor and the measurements are described in the Dutch report R 343 D (ref. 1) of which the title can be translated as: "Report of wind tunnel measurements performed on a 2-bladed rotor with blades made out of a cylinder". This report is no longer available but in November 2016 I have made an English translation of the parts out of report R 343 D about the rotor with 2 mm stainless steel blades and a design tip speed ratio $\lambda_d = 6$. This translation has report number KD 616 (ref. 2).

In 1978 I was working as a technical designer of water pumping windmills, pumps and test rigs at the Wind Energy Group of the University of Technology Eindhoven. This group was a member of CWD, Consultancy services Wind energy Developing countries. The measurements have been performed in the open wind tunnel of TNO Waddinxveen. TNO was a member of CWD during the first five years of CWD. This wind tunnel is later moved to the University of Delft and I have measured several other rotors in this wind tunnel. The wind tunnel is blowing air into the open space and the wake therefore can expand around the rotor which also happens in real wind. So there is no tunnel blockage as it is the case for closed wind tunnels. The measurements are therefore very accurate. The wind tunnel has a diameter of 2.2 m and the maximum rotor diameter of a rotor which can be measured is 1.8 m. All measured rotors as described in R 343 D have a diameter of 1.8 m.

It was rather difficult and expensive to manufacture the measured rotor. In chapter 5 of KD 616, a slightly larger rotor with a diameter of 2.02 m is described which also makes use of 2 mm stainless steel for the blades but for which the blades are connected to the generator hub by a simple twisted and cambered connecting strip.

A larger 2-bladed rotor with tapered blades and a rotor diameter of 2.92 m is described in report KD 656 (ref. 3). This rotor is coupled to the VIRYA-2.68 PM-generator. It seems possible to use a similar construction for an even bigger rotor which is coupled to the VIRYA-4.2 PM-generator. It appears that this is the case for a rotor diameter of 3.9 m and the windmill is therefore called the VIRYA-3.9.

The measurements of the VIRYA-4.2 generator are given in report KD 200 (ref. 4). The VIRYA-3.9 will be used for 24 V battery if the original 230/400 V winding of the generator is rectified in delta. The VIRYA generators are described in report KD 341 (ref. 5). The generator is based on an asynchronous 3-phase motor of manufacture ROTOR type 5RN112M04V (frame size 112 with lengthened stator iron) for which the short-circuit armature is replaced by an armature provided with permanent magnets. The drawing of the VIRYA-4.2 generator is not public.

The original VIRYA-4.2 has a 2-bladed rotor with wooden blades. It might be difficult to get the needed quality of wood and machining of wood might be not common for an average workshop. Wooden blades can also been damaged easily during transport. Therefore it is investigated if an alternative rotor with stainless steel blades can be used. The VIRYA-3.9 has a somewhat smaller rotor diameter than the original VIRYA-4.2 but it is assumed that the head geometry of the VIRYA-4.2 can be maintained. The effect of the slightly smaller rotor diameter of the VIRYA-3.9 on the rotor thrust is compensated because rotors with cambered steel blades have a slightly larger thrust coefficient (about 0.75 in stead of 0.7). So the head and the tower are the same as the head and tower of the VIRYA-4.2. This head results in a rated wind speed of about 11 m/s.

2 Description of the rotor of the VIRYA-3.9 windmill

The 2-bladed rotor of the VIRYA-3.9 windmill has a diameter D = 3.9 m and a design tip speed ratio λ_d = 6. Advantages of a 2-bladed rotor are that no welded spoke assembly is required and that the rotor can be balanced and transported easily, even if it is mounted.

The rotor has tapered blades which are made out of a cylinder. The camber is therefore small at the blade tip and large at the blade root. In the first instance, the blade geometry is chosen such that the blade is scaled as good as possible to the blades of the 1.8 m rotor which was tested in the wind tunnel. The scale factor is 3.9 / 1.8 = 2.1667. The original 1.8 m rotor had a sheet width at the blade tip of 75 mm, so the sheet width of a VIRYA-3.9 blade should be about 75 * 2.1667 = 162.5 mm. However, a larger width of 180 mm is chosen because this matches better with the available sheet size and because this results in a somewhat lower lift coefficient.

The free blade length of the original 1.8 m rotor was 0.8 m for 2 mm stainless steel sheet. As freely supported cambered steel blades are sensible to flutter at high wind speeds, the free blade length should have a certain ratio with the sheet thickness. So if the sheet thickness is increased by a factor 1.5 from 2 mm up to 3 mm, the free blade length can also be increased by a factor 1.5 from 0.8 m up to 1.2 m.

It is decided to use 3 mm stainless steel sheet size 1500 * 3000 mm for the blades. It is decided that there is an overlap of 300 mm = 0.3 m in between a blade and the connecting strip. This means that the free blade length is 1.2 m. This seems acceptable.

A sheet size 1500 * 3000 mm is cut into six sheets size 500 * 1500 mm. Cambering of tapered blades is difficult as it requires a complicated press. Cambering of a rectangular sheet is easier and it can be done with a hydraulic blade press similar to the blade press which is used for constant chord blades. So the rectangular sheet is cambered with the correct radius. The two tapered blades are made out of this cambered sheet by a rectangular grinder.

Assume that the groove made by the rectangular grinder has a width of 3 mm This means that if the width at the blade tip is chosen 180 mm, the width at the blade root will be 500 – 180 – 3 = 317 mm. So the increase of the width from the blade tip up to the blade root is 317 – 180 = 137 mm. This results in a taper angle of the blade of 5.2°. The taper angle of the blades of the original 1.8 m rotor is 4.74°. So the taper angle is 0.46° larger which is acceptable.

The camber radius of the original blades is 150 mm. So the radius of the VIRYA-3.9 blades should be about 2.1667 * 150 = 325 mm. However, the sheet width was chosen larger than according to scaling with a factor 2.1667. The camber radius is therefore also chosen larger. The camber radius of the VIRYA-2.92 is 290 mm. These blades are made out of a rectangular sheet size 375 * 1250 mm. So the sheet used for the VIRYA-3.9 is a factor 1500 / 1250 = 1.2 larger. If this factor is also used for the camber radius, the camber radius should be 1.2 * 290 = 348 mm. Finally it is chosen that the camber radius = 350 mm. The airfoil nose and the tailing edge of the blade have to be rounded with a radius of at least 1 mm to minimise drag.

The connecting strip has dimensions 100 * 10 * 1500 mm. The overlap in between blade and strip is 300 mm. The distance in between the heart of the strip and the tailing edge of the blade is chosen 145 mm. The connecting strip is twisted 13° in between the hub and the blade root to realize the correct blade setting angle at the blade root.

A blade is connected to the strip by three bolts M12. The strip is bevelled 5° at the left and the right back side over a length of 300 mm to prevent that the camber of the blade is flattened when the bolts are tightened. The hub has an outer diameter of 80 mm. The connecting strip is connected to the hub by two bolts M12. The hub is connected to the tapered shaft of the generator by one central bolt M16.

3 Calculation of the rotor geometry

The original 1.8 m rotor was calculated but the calculations are lost as they are not mentioned in report R 343 D. However, the result of the calculation is given in a table which is mentioned on the manufacturing drawing of the rotor. A reduced copy of this drawing is given in figure 1 of KD 616 (ref. 2). The rotor calculations were made for only four stations. Six stations will be chosen for the VIRYA-3.9 rotor. These stations are called A, B, C, D, E and F and for the corresponding local radii r it is chosen that r_A = 1.95 m, r_B = 1.65 m, r_C = 1.35 m, r_D = 1.05 m, r_E = 0.75 m and r_F = 0.45 m. Station E corresponds to the end of the connecting strip. Station F corresponds to the blade root. The direction of numbering is just opposite that of the original 1.8 m rotor but the chosen direction is the same as for all other VIRYA rotors.

A problem with making of the rotor calculations for the VIRYA-3.9 rotor is that the camber is different for each station. The chord c and the camber C of each station can be calculated using the formulas given in chapter 5 of report KD 398 (ref. 6) but for the rotor calculations one needs aerodynamic characteristics for different camber. In KD 398 these characteristics are given only for 7.14 %, 10 % and 12.5 % camber.

The sheet width b can be calculated easily for the six chosen stations as the flat sheet is tapered linear. However, the chord c is smaller than the sheet width b and how much smaller depends on the camber. The sheet width was chosen 180 mm at the blade tip (at r_A = 1.95 m) and 317 mm at the blade root (at r_F = 0.45 m). So the difference is 137 mm. This means that the sheet width b increases 137 / 5 = 27.4 mm per station. This gives the following values: b_A = 180 mm, b_B = 207.4 mm, b_C = 234.8 mm, b_D = 262.2 mm, b_E = 289.6 mm and b_F = 317 mm. The camber radius was chosen 350 mm.

The formulas which give the relation in between the strip width b, the chord c, the camber radius r_c, the airfoil thickness a, the half camber angle α_c and the camber C are given in chapter 5 of report KD 398 (ref. 6). Figure 8 of KD 398 gives the geometry of a cambered plate. The calculations can be made on a pocket calculator if it is put in the modulus “rad”. The strip width b and the bending radius r_c is known. We want to calculate the chord c and the camber C. First we have to calculate the half camber angle α_r which is given by formula 1 of KD 398. Next c is calculated with formula 5 of KD 398. Next C is calculated with formula 6 of KD 398. The result of the calculations is given in table 1.

Station	b (mm)	r_c (mm)	α_c (rad)	c (mm)	c (m)	C (%)
A	180	350	0.2571	178.0	0.178	6.46
B	207.4	350	0.2963	204.4	0.2044	7.46
C	234.8	350	0.3354	230.4	0.2304	8.46
D	262.2	350	0.3746	256.1	0.2561	9.48
E	289.6	350	0.4137	281.4	0.2814	10.49
F	317	350	0.4529	306.3	0.3063	11.52

table 1 Calculated values of the chord c and the camber C for different stations

The rotor geometry is determined using the method and the formulas as given in report KD 35 (ref. 7). This report (KD 733) has its own formula numbering. Substitution of λ_d = 6 and R = 1.95 m in formula (5.1) of KD 35 gives:

$$\lambda_{r\,d} = 3.0769 * r \qquad (-) \qquad (1)$$

Formula’s (5.2) and (5.3) of KD 35 stay the same so:

$$\beta = \phi - \alpha \qquad (°) \qquad (2)$$

$\phi = 2/3 \arctan 1 / \lambda_{r\,d}$ (°) (3)

Substitution of B = 2 in formula (5.4) of KD 35 gives:

$C_l = 12.566 * r (1 - \cos\phi) / c$ (-) (4)

Substitution of V = 5 m/s in formula (5.5) of KD 35 gives:

$R_{e\,r} = 3.335 * 10^5 * c * \sqrt{(\lambda_{r\,d}^2 + 4/9)}$ (-) (5)

The blade is calculated for six stations A till F which have a distance of 0.3 m of one to another. The blade has a chord which increases at decreasing radius and the calculations therefore correspond with the example as given in chapter 5.4.1 of KD 35. This means that the lift coefficient should be about constant and about equal to the optimum lift coefficient for the whole blade. First the theoretical values are determined for C_l, α and β. Next the real blade angle β_{real} is determined for the chosen blade taper using figure 1. The result of the calculations is given in table 2. The aerodynamic characteristics of cambered airfoils are given in report KD 398 (ref. 6). The Reynolds values for the stations are calculated for a wind speed of 5 m/s because this is a reasonable wind speed for a windmill with V_{rated} = 11 m/s. Those airfoil Reynolds numbers are used which are lying closest to the calculated values.

sta-tion	r (m)	λ_{rd} (-)	ϕ (°)	c (m)	$C_{l\,th}$ (-)	$R_{e\,r} * 10^{-5}$ V = 5 m/s	Camber C (%)	Camber used (%)	$R_e * 10^{-5}$	α_{th} (°)	β_{th} (°)	β_{real} (°)
A	1.95	6	6.3	0.178	0.83	3.58	6.46	7.14	3.4	0.5	5.8	4
B	1.65	5.077	7.4	0.2044	0.85	3.49	7.46	7.14	3.4	0.7	6.7	6.2
C	1.35	4.154	9.0	0.2304	0.91	3.23	8.46	7.14 + 10	3.4	0.7	8.3	8.4
D	1.05	3.231	11.5	0.2561	1.03	2.82	9.48	10	2.5	0.8	10.7	10.6
E	0.75	2.308	15.6	0.2814	1.24	2.25	10.49	10	2.5	2.3	13.3	12.8
F	0.45	1.385	23.9	0.3063	1.58	1.57	11.52	12.5	1.7	6.7	17.2	15.0

table 2 Calculation of the blade geometry of the VIRYA-3.9 rotor

In table 2 it can be seen that the theoretical lift coefficient C_{lth} is not constant but increasing at decreasing values of r. But the increase is less than for a constant chord blade.

The camber is increasing from 6.46 % at station A to 11.52 % at station F. To find the theoretical angles of attack α_{th} we need C_l-α curves for the six different cambers. However, only characteristics for 7.14 %, 10 % and 12.5 % are available. The C_l-α curve for 7.14 % camber was used for station A and B. The average angle of the C_l-α curves for 7.14 % and 10 % camber was used for station C. The C_l-α curve for 10 % camber was used for stations D and E. The C_l-α curve for 12.5 % camber was used for station F.

In table 1 it can be seen that the theoretical blade angles β_{th} vary in between 5.8° at the blade tip and 17.2° at station F. In the table at figure 1 of report KD 616 it can be seen that the blade angle at the blade tip is only 2.1°, so much smaller than 5.8°. A problem with a rotor made out of a cylinder is that only the blade angle at the blade tip β_A can be adjusted at a certain value. The blade angles at other stations depend on the taper of the blade and are difficult to calculate for a certain value of β_A. They are given on the composite drawing of the cross sections of the 1.8 m rotor which is given at the right side in figure 1 of KD 616. A similar composite drawing was made for the six stations of a VIRYA-3.9 blade for different values of β_A. The composite drawing for the right blade seen from the right side is given as figure 1. It was found that β_A = 4° gives real values of β for the sections B, C, D, E and F which are matching best with the calculated values of β_{th} in table 2.

The values for β found from the composite drawing are given in table 2 as β_{real}. The angle for which the connecting strip has to be twisted right hand is 13° for β_A = 4°. A sketch of the whole rotor is given in figure 2.

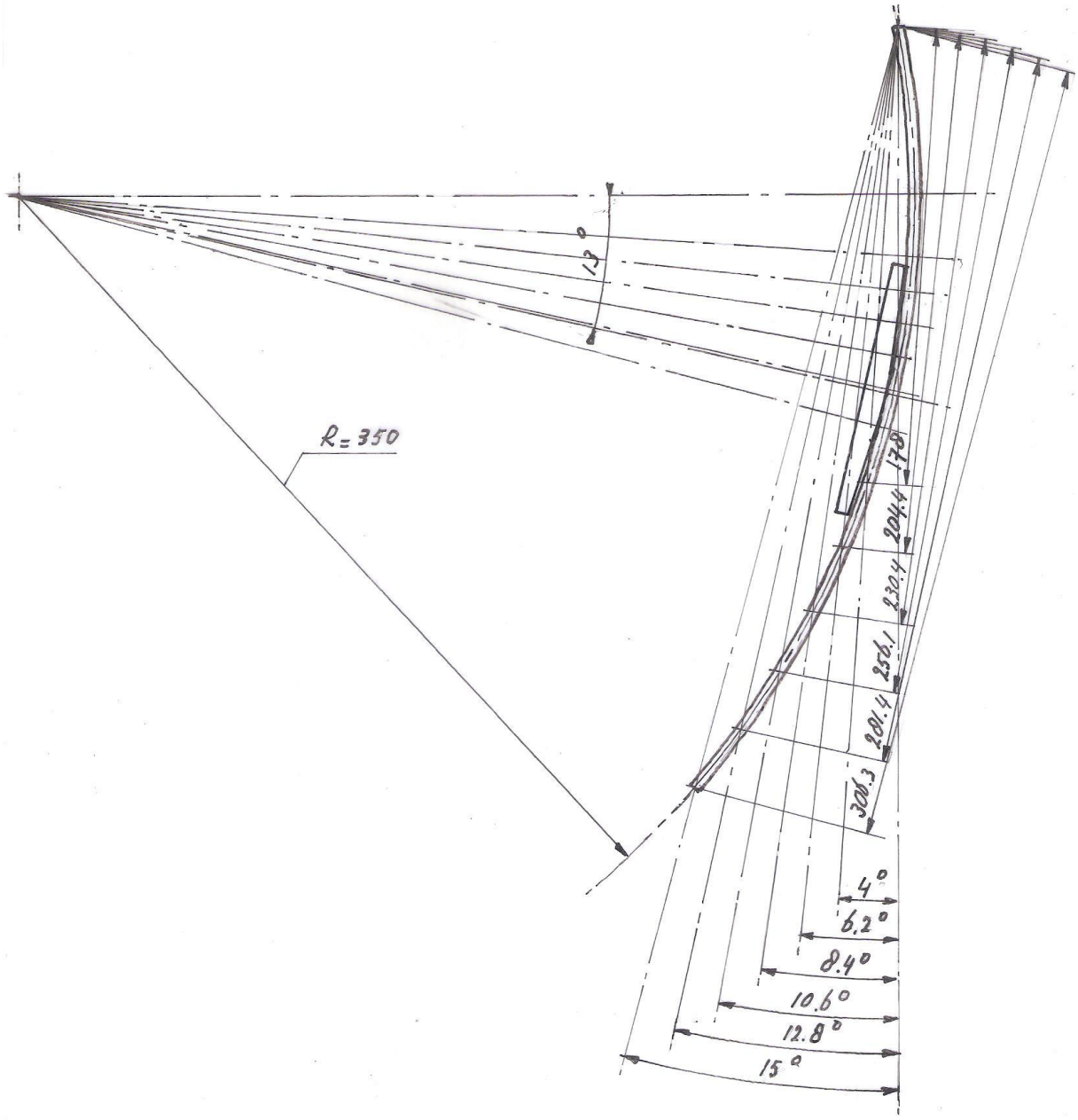

fig. 1 The right blade for six stations A, B, C, D, E and F

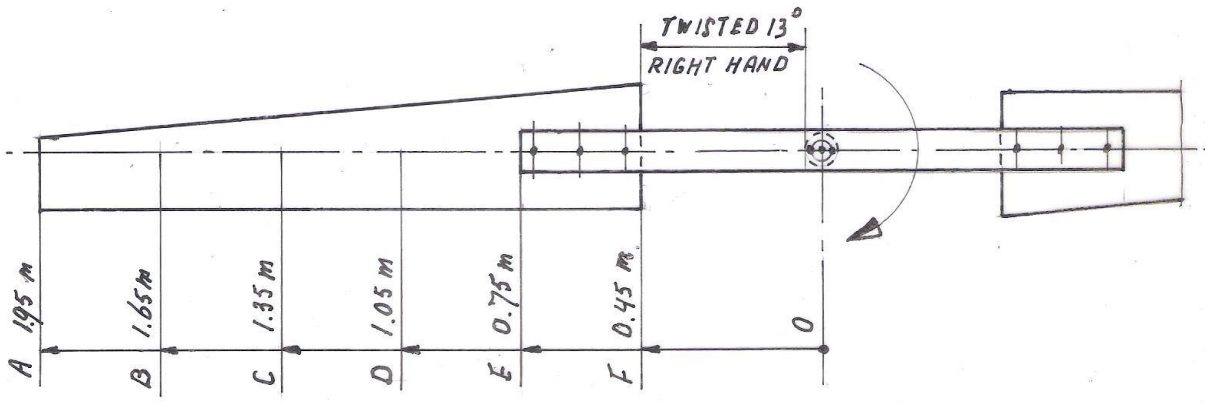

fig. 2 Front view of the VIRYA-3.9 rotor

4 Determination of the C_p-λ and the C_q-λ curves

The determination of the C_p-λ and C_q-λ curves is given in chapter 6 of KD 35. However, the original 1.8 m diameter rotor has been measured in the wind tunnel and the measured characteristics should be more accurate than estimated ones. The wind tunnel measurements for the rotor with 2 mm stainless steel blade were only performed for a wind tunnel speed of 11 m/s which results in rather high Reynolds values. The VIRYA-3.9 is a factor 2.167 larger than the tested rotor. However, the chord at the blade tip is relatively a factor 180 / 162.5 = 1.108 larger. This means that the Reynolds value is a factor 2.167 * 1.108 = 2.4 larger for a wind speed of 11 m/s. So the Reynolds value is the same for a wind speed of 11 / 2.4 = 4.6 m/s. This is even smaller than the value of 5 m/s which was used for the rotor calculations.

The measured C_p-λ and C_q-λ curves are given in figure 2 and 3 of KD 616. The C_p is about 0.41 for $\lambda = 6$. However, there is an unusual peak in the C_p-λ curve for $6.3 < \lambda < 7.5$. A similar rotor made out of 2 mm aluminium sheet has been measured for a tunnel speed of 5.5 m/s and then there is no unusual peak in the C_p-λ curve. So the peak must be caused by Reynolds effects and is explained in KD 616 as the result of the special shape of the C_l-α curve of a 10 % cambered airfoil as measured by Volkers.

For the VIRYA-3.9 it is assumed that the C_p-λ curve has no unusual peak at higher tip speed ratios and that the maximum $C_p = 0.41$ for $\lambda_d = 6$. As the VIRYA-3.9 rotor has chords which are relatively larger than those of the 1.8 m original rotor and as the blade angle at the tip is 4° in stead of 2.1° it is assumed that the starting torque coefficient is 0.0075 in stead of 0.005. The estimated C_p-λ and C_q-λ curves are given in figure 3 and 4. The curves are made about similar to the measured curves except for the unusual peak and the starting torque coefficient. But for high wind speeds, the peak will certainly exist. If the rotor is running in the peak area it will produce more power and it will make very little noise.

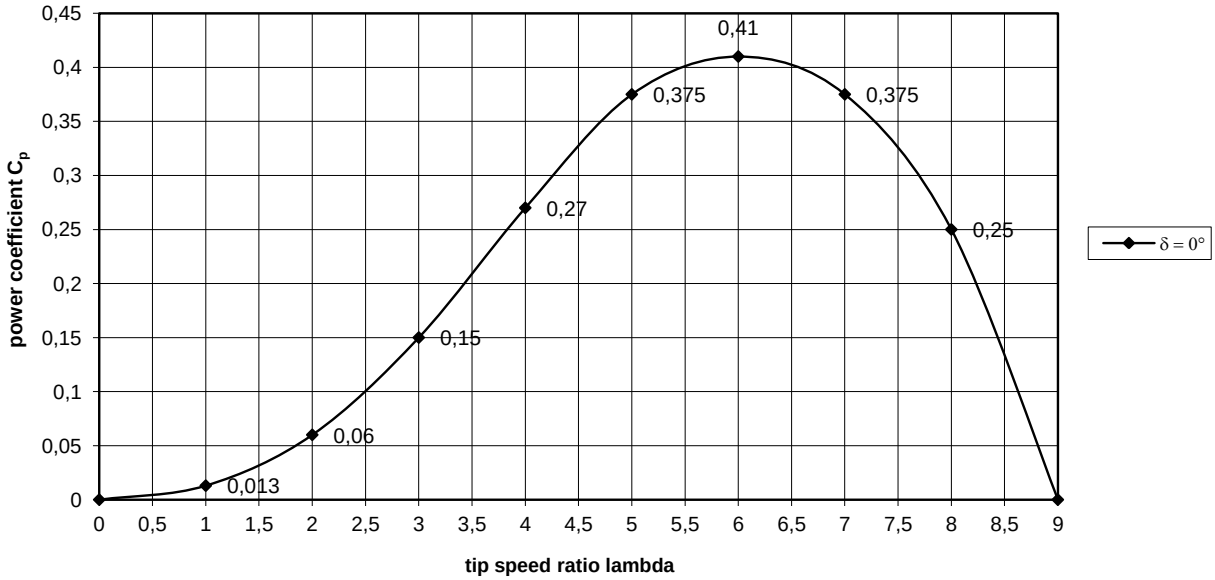

fig. 3 Estimated C_p-λ curve for the VIRYA-3.9 rotor for the wind direction perpendicular to the rotor ($\delta = 0°$)

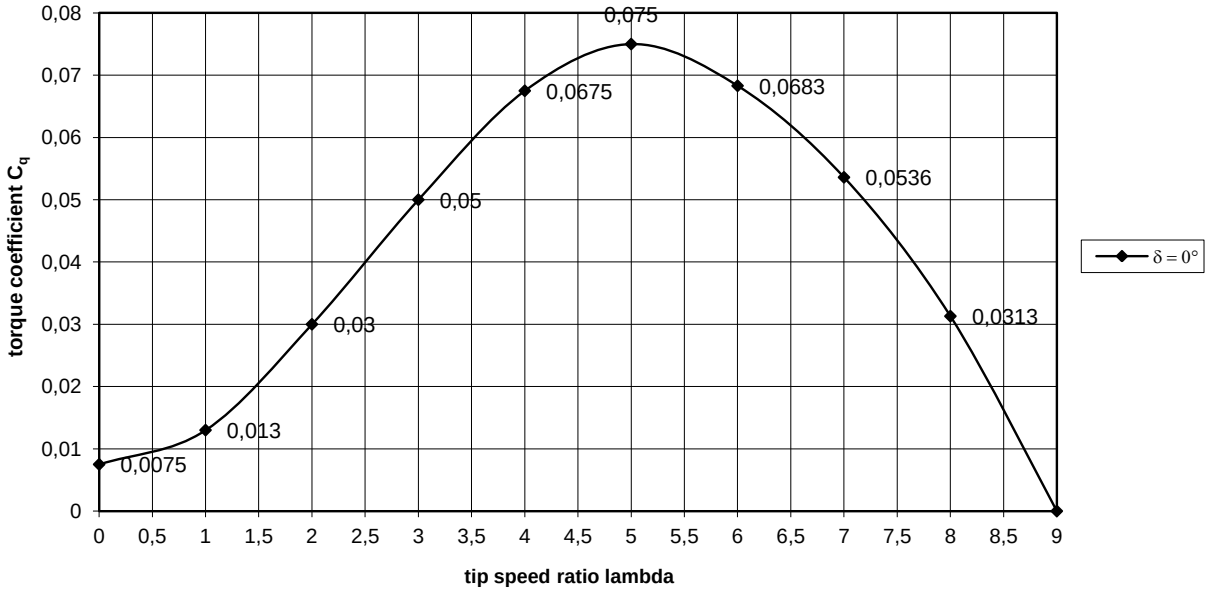

fig. 4 Estimated C_q-λ curve for the VIRYA-3.9 rotor for the wind direction perpendicular to the rotor (δ = 0°)

In figure 4 it can be seen that for the starting torque coefficient it is valid that $C_{qstart} = 0.0075$. The starting wind speed V_{start} of the rotor is calculated with formula 8.6 of KD 35 which is given by:

$$V_{start} = \sqrt{\left(\frac{Q_s}{C_{q\,start} * ½\rho * \pi R^3}\right)} \quad \text{(m/s)} \qquad (6)$$

For the VIRYA-4.2 generator, a sticking torque Q_s has been measured of about 0.9 Nm if the shaft is not rotating. Substitution of $Q_s = 0.9$ Nm, $C_{q\,start} = 0.0075$, $\rho = 1.2$ kg/m^3 and $R = 1.95$ m in formula 6 gives that $V_{start} = 2.9$ m/s. This is acceptable low for a 2-bladed rotor with a design tip speed ratio of 6. If the generator is used in delta for 24 V battery charging, the unloaded Q-n curve is rising faster than for star rectification because higher harmonic currents can circulate in the winding. However, the Q-n curve of the rotor is also rising rather fast and therefore the real starting wind speed will be about the same as the calculated value. This will be checked in chapter 6.

5 Determination of the P-n curves and the P_{el}-V curve for 26 V delta and 26 V star

The determination of the P-n curves of a windmill rotor is described in chapter 8 of KD 35. One needs a C_p-λ curve of the rotor and a δ-V curve of the safety system together with the formulas for the power P and the rotational speed n. The C_p-λ curve is given in figure 3. The δ-V curve of the safety system depends on the vane blade mass per area. The vane blade is made of 9 mm meranti waterproof plywood with a density of about 0.6 *10^3 kg/m^3. This vane blade gives a rated wind speed V_{rated} of about 11 m/s. In report KD 223 (ref. 8) a method is given to check the estimated δ-V curve and the estimated δ-V curve of the VIRYA-3.3D windmill is checked as an example. This windmill also has a vane blade made of 9 mm plywood. So the δ-V curve of the VIRYA-3.3D will be about the same as for the VIRYA-3.9. The estimated and calculated curves appear to lie very close to each other so it is allowed to use the estimated curve. The estimated curve is given in figure 5.

The head starts to turn away at a wind speed of about 5 m/s. For wind speeds above 11 m/s it is supposed that the head turns out of the wind such that the component of the wind speed perpendicular to the rotor plane, is staying constant. The P-n curve for 11 m/s will therefore also be valid for wind speeds higher than 11 m/s.

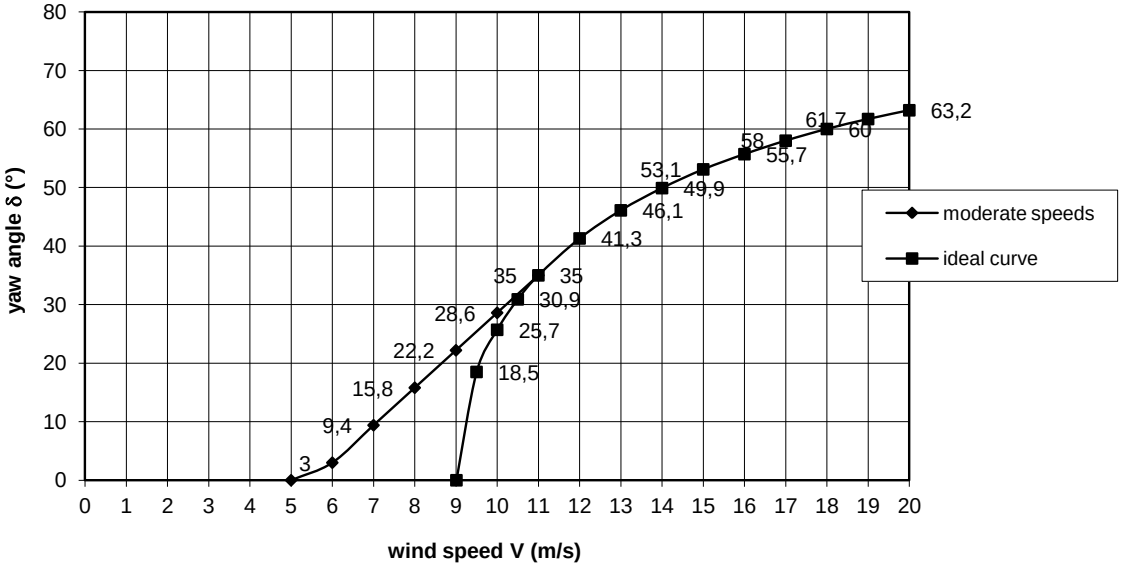

fig. 5 Estimated δ-V curve for a 9 mm plywood vane blade

The P-n curves are determined for wind the speeds 3, 4, 5, 6, 7, 8, 9, 10, and 11 m/s. At high wind speeds the rotor is turned out of the wind by a yaw angle δ and therefore the formulas for P and n are used which are given in chapter 7 of KD 35.

Substitution of R = 1.95 m in formula 7.1 of KD 35 gives:

$$n_\delta = 4.8971 * \lambda * \cos\delta * V \qquad \text{(rpm)} \qquad (7)$$

Substitution of $\rho = 1.2$ kg / m^3 and R = 1.95 m in formula 7.10 of KD 35 gives:

$$P_\delta = 7.1675 * C_p * \cos^3\delta * V^3 \qquad \text{(W)} \qquad (8)$$

The P-n curves are determined for C_p values belonging to λ is 3, 4, 5, 6, 7, 8 and 9 (see figure 3). For a certain wind speed, for instance V = 3 m/s, related values of C_p and λ are substituted in formula 7 and 8 and this gives the P-n curve for that wind speed. For the higher wind speeds the yaw angle as given by figure 5, is taken into account. The result of the calculations is given in table 3.

		V = 3 m/s δ = 0°		V = 4 m/s δ = 0°		V = 5 m/s δ = 0°		V = 6 m/s δ = 3°		V = 7 m/s δ = 9.4°		V = 8 m/s δ = 15.8°		V = 9 m/s δ = 22.2°		V = 10 m/s δ = 28.6°		V = 11 m/s δ = 35°	
λ (-)	C_p (-)	n (rpm)	P (W)	n (rpm)	P (W)	n (rpm)	P (W)	n_δ (rpm)	P_δ (W)	n_δ (rpm)	P_δ (W)	n_δ (rpm)	P_δ (W)	n_δ (rpm)	P_δ (W)	n_δ (rpm)	P_δ (W)	n_δ (rpm)	P_δ (W)
3	0.15	44.1	29	58.8	69	73.5	134	88.0	231	101.5	354	113.1	490	122.4	622	129.0	728	132.4	787
4	0.27	58.8	52	78.4	124	97.9	242	117.4	416	135.3	637	150.8	883	163.2	1120	172.0	1310	176.5	1416
5	0.375	73.5	73	97.9	172	122.4	336	146.7	578	169.1	885	188.5	1226	204.0	1555	215.0	1819	220.6	1966
6	0.41	88.1	79	117.5	188	146.9	367	176.1	632	202.9	968	226.2	1340	244.8	1700	258.0	1989	264.8	2150
7	0.375	102.8	73	137.1	172	171.4	336	205.4	578	236.7	885	263.9	1226	285.6	1555	301.0	1819	308.9	1966
8	0.25	117.5	48	156.7	115	195.9	224	234.7	385	270.6	590	301.6	817	326.5	1037	344.0	1213	353.0	1311
9	0	132.2	0	176.3	0	220.4	0	264.1	0	304.4	0	339.3	0	367.3	0	387.0	0	397.1	0

table 3 Calculated values of n and P as a function of λ and V for the VIRYA-3.9 rotor

The calculated values for n and P are plotted in figure 6. The optimum cubic line which is going through the tops of the P-n curves is also given in figure 6.

The 4-pole generator of the VIRYA-4.2 windmill has been measured in delta for a constant voltage of 26 V which is the average charging voltage of a 24 V battery. The measurements were performed for the original 230/400 V winding. The measured P_{mech}-n and the P_{el}-n curves for U = 26 V delta are also plotted in figure 6. The generator has not been measured for 26 V star but the characteristics for 26 V star are estimated in chapter 5 of report KD 200 (ref. 4). The estimated P_{mech}-n and the P_{el}-n curves for U = 26 V star are also plotted in figure 6.

The generator has been measured for short-circuit in delta because the maximum torque level for short-circuit in delta is higher than for short-circuit in star. The P-n curve for short-circuit in delta is also plotted in figure 6.

The point of intersection of the P_{mech}-n curve of the generator with the P-n curve of the rotor for a certain wind speed, gives the working point for that wind speed. The electrical power P_{el} for that wind speed is found by going down vertically from the working point up to the point of intersection with the P_{el}-n curve. The values of P_{el} found this way for all wind speeds, are plotted in the P_{el}-V curves (see figure 7) for 26 V delta and for 26 V star.

The matching of rotor and generator for 26 V delta is rather good because the P_{mech}-n curve of the generator is lying only somewhat to the right from the optimum cubic line for wind speeds higher than 4 m/s. The real tip speed ratio for wind speeds around 7 m/s is about 6.5. This is just the tip speed ratio for which the original 1.8 m rotor had a peak in the C_p-λ curve and for which the rotor was very silent. It is expected that this is also the case for the VIRYA-3.9 rotor and this rotor in combination with the VIRYA-4.2 generator for 26 V delta will therefore be much more silent than rotors with steel blades with a high tip speed ratio and a constant chord.

The matching of rotor and generator for 26 V star is also rather good because the P_{mech}-n curve of the generator is lying only somewhat to the left from the optimum cubic line for wind speeds in between 3 m/s and 7 m/s. However, for high wind speeds, the load isn't strong enough and for V = 11 m/s, the P_{mech}-n curve for 26 V star is lying even more to the right than the P_{mech}-n curve for 26 V delta.

In the P_{el}-V curve for 26 V delta it can be seen that the maximum power is 910 W at a wind speed of 11 m/s. The supply of power starts at a wind speed of 3.2 m/s ($V_{cut\ in}$ = 3.2 m/s). In chapter 4 it was calculated that V_{start} = 2.9 m/s so there is no hysteresis in the P_{el}-V curve for 26 V delta.

In the P_{el}-V curve for 26 V star it can be seen that the maximum power is 670 W at a wind speed of 11 m/s which is a lot lower than for 26 V delta. This is because the generator efficiency is a lot lower at high currents for 26 V star than for 26 V delta. The supply of power starts at a wind speed of 2.4 m/s ($V_{cut\ in}$ = 2.4 m/s). In chapter 4 it was calculated that V_{start} = 2.9 m/s so there is hysteresis in the P_{el}-V curve for 26 V star for 2.4 m/s < V < 2.9 m/s.

If both P_{el}-V curves are compared it can be seen that the curve for 26 V star is better for wind speeds below 5 m/s but that the curve for 26 V delta is much better above 5 m/s. So 26 V star is only advised for regions with low wind speeds.

As at high wind speeds, the electrical power for 26 V star is much lower than for 26 V delta, it means that more heat is generated in the winding for 26 V star. So it must be investigated if the generator isn't becoming too hot at high wind speeds for 26 V star. If it appears that the generator becomes too hot at high wind speeds, the maximum power can be reduced by taking a lighter vane blade.

The P-n curve for short-circuit in delta is lying just above the P-n curve of the rotor for V = 9 m/s. So the rotor will only slow down to almost stand still if short-circuit in delta is made and if the wind speed is less than 9 m/s.

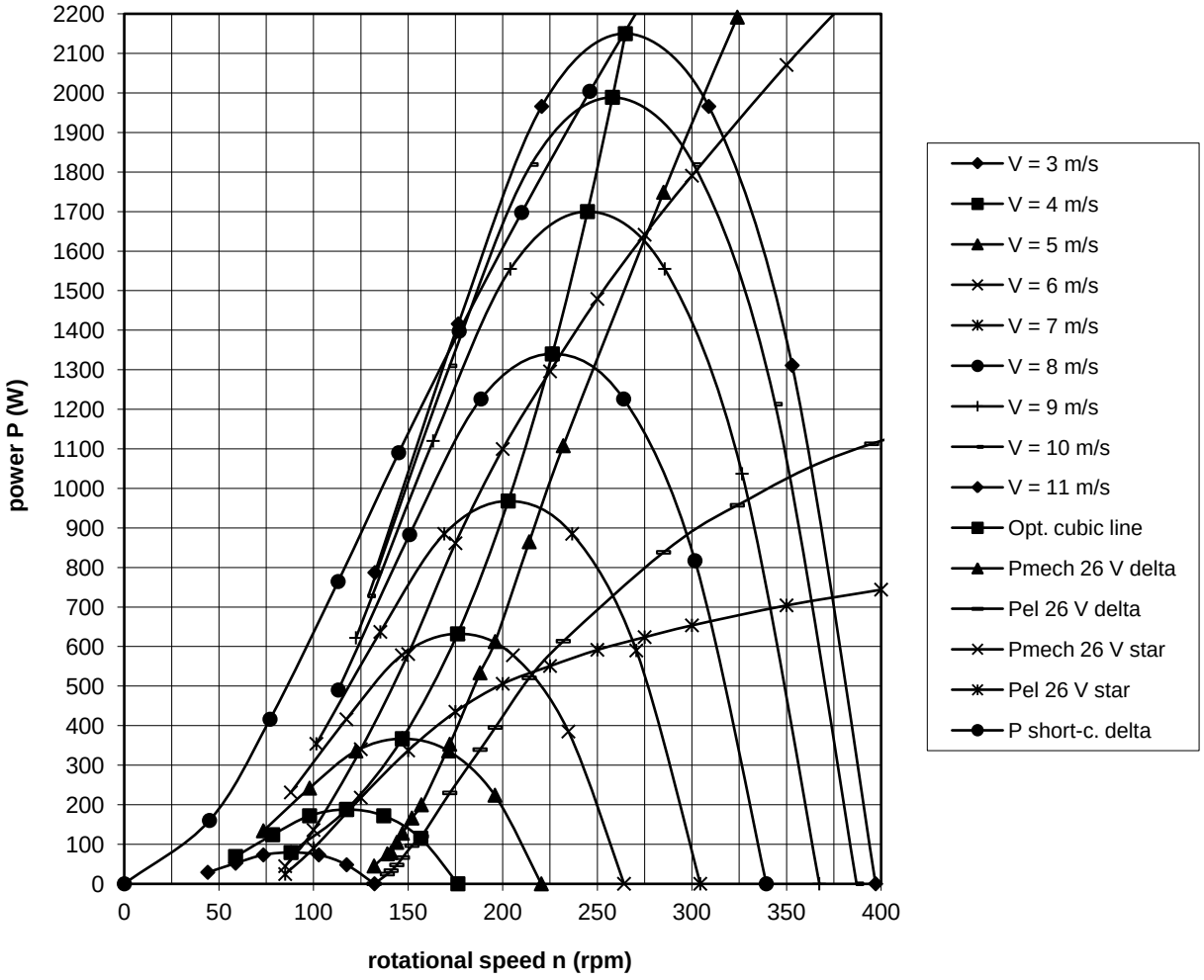

fig. 6 P-n curves of the VIRYA-3.9 rotor and the generator for 26 V delta and 26 V star

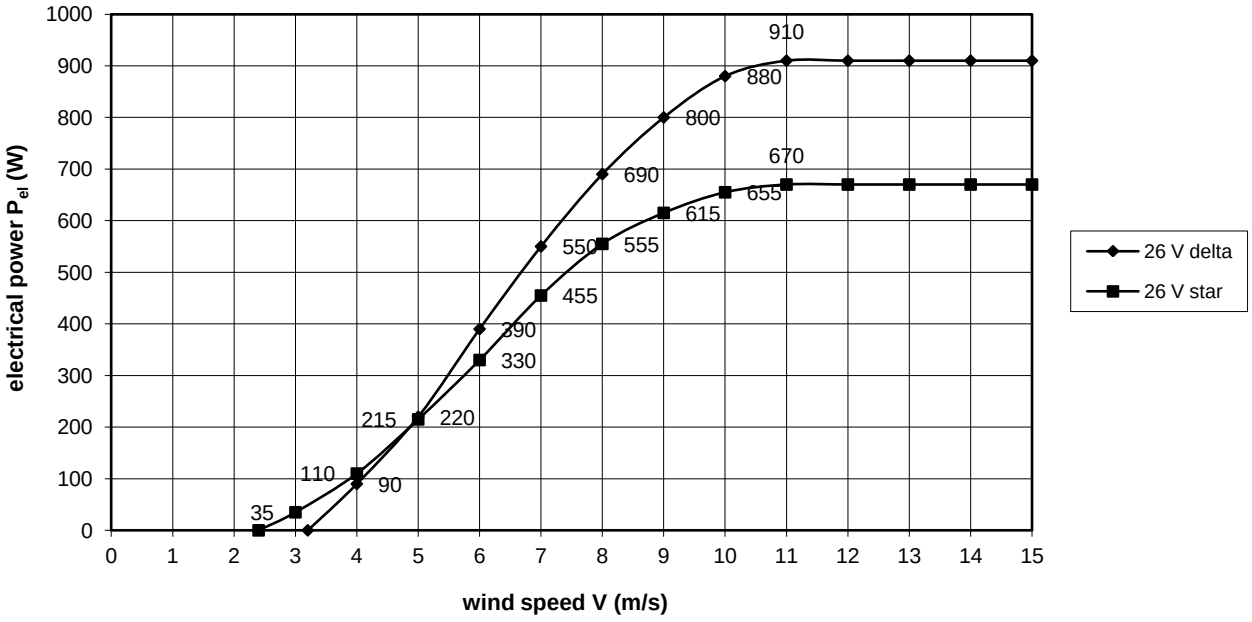

fig. 7 P_{el}-V curve of the VIRYA-3.9 windmill for 26 V delta and 26 V star

6 Checking of the starting behaviour

In chapter 4 it has been calculated that the starting wind speed is 2.9 m/s. At this wind speed the rotor is able to generate the unloaded sticking torque of 0.9 Nm of the generator if the shaft is not rotating. The unloaded sticking torque increases at increasing rotational speeds but how much depends on how the generator is rectified. The sticking torque for delta rectification rises faster than for star rectification because higher harmonic currents can circulate in the winding for delta rectification. The sticking torque has been measured for both situations and the result is given in figure 1 of report KD 200. This figure is copied as figure 8 for low rotational speeds.

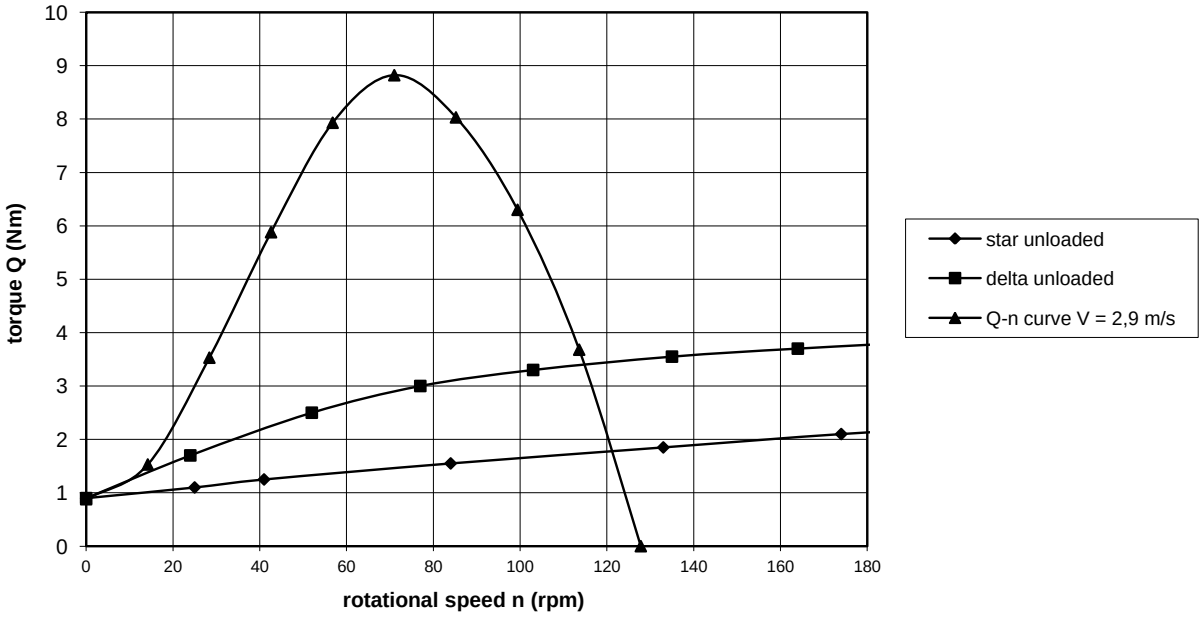

fig. 8 Unloaded sticking torque of the generator for rectification in delta and star and Q-n curves of the rotor for V = 2.9 m/s

The Q-n curve of the rotor for a certain wind speed can be determined in the same way as the P-n curve for a certain wind speed but one has to use the formula for Q in stead as the formula for P. The formula for Q for a rotor perpendicular to the wind is given by formula 4.3 of KD 35. Substitution of $\rho = 1.2$ kg/m^3, V = 2.9 m/s and R = 1.95 m in this formula gives:

$$Q = 117.54 * C_q \qquad \text{(Nm)} \qquad (9)$$

The rotational speed n is given by formula 7. Substitution of $\delta = 0°$ and V = 2.9 m/s in formula 7 gives:

$$n = 14.202 * \lambda \qquad \text{(rpm)} \qquad (10)$$

The Q-n curve is now determined for values λ of 0, 1, 2, 3, 4, 5, 6, 7, 8 and 9 and the corresponding values of C_q (see figure 2). The Q-n curve found this way is also given in figure 8. In figure 8 it can be seen that the Q-n curve for V = 2.9 m/s is rising faster than the unloaded sticking torque for rectification in star. However, at low rpm, it is rising with about the same rate as the unloading sticking torque for rectification in delta. This means that at V = 2.9 m/s, there is no torque difference to accelerate the rotor. So the real starting wind speed will be a little higher than 2.9 m/s if the generator is rectified in delta. This is certainly acceptable and so use of the VIRYA-3.9 rotor in combination with the VIRYA-4.2 generator for 26 V delta is a realistic option.

7 Use of a modified 115/200 V winding for 26 V star

The generator has been measured for the original 230/400 V winding. It is possible to modify this winding into a 115/200 V winding by connecting the first and the second layer in parallel in stead of in series. This results in halving of the voltage and in doubling of the current. The modification procedure is described in chapter 4 of report KD 341 (ref. 5).

The generator has been measured for 52 V star. This is the average charging voltage of a 48 V battery. The original VIRYA-4.2 was used for 48 V battery charging and so the measurements for 52 V star could be used. However, a battery voltage of 48 V is less common than 24 V and a special 55.2 V battery charge controller has to be used to limit the maximum charging voltage up to 2.3 V per cell. A 27.6 V, 200 W battery charge controller is described in a manual which is available on my website at the bottom of the list with KD-reports (ref. 9). The power which can be dissipated can be increased to 1200 W by connecting six dump load modules together in parallel.

So now it is assumed that the standard 230/400 V winding is modified into a 115/200 V winding. The measured characteristics for 52 V star can now be used for 26 V star. Figure 6 is now copied as figure 9 but the curves for the original winding for 26 V delta and 26 V star are replaced by the curves for the modified winding for 26 V star.

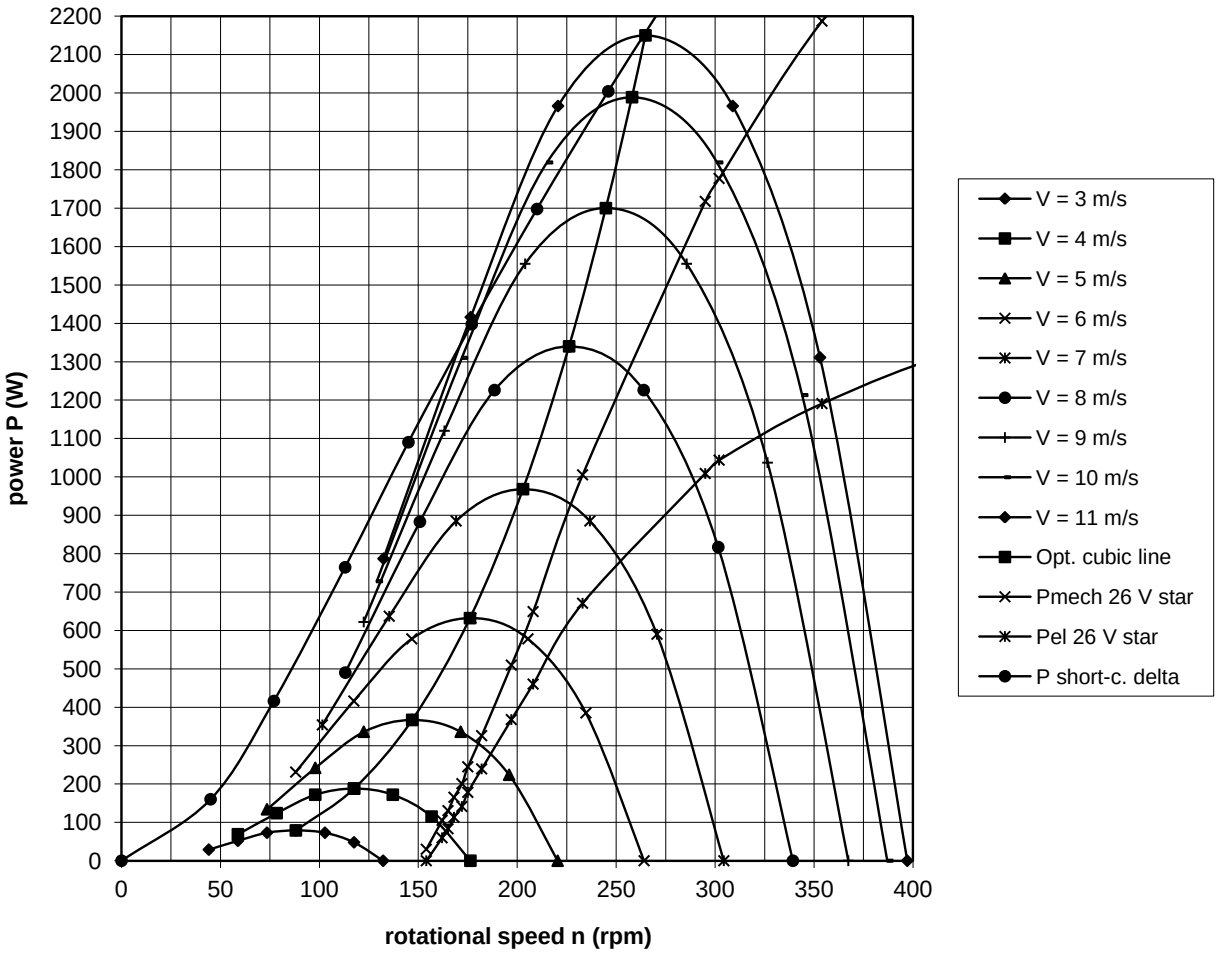

fig. 9 P-n curves of the VIRYA-3.9 rotor and the generator for 26 V star for the modified 115/200 V winding

Is figure 9 is compared with figure 6 it can be seen that the P_{mech}-n curve for the modified winding for 26 V star is lying somewhat more to the right than the P_{mech}-n curve for the original winding for 26 V delta. So the matching is less good but still acceptable.

The noise production will still be low because the rotor runs with a tip speed ratio for which the original 1.8 m rotor was very silent. The P_{el}-V curve for the modified winding for 26 V star is derived in the same way as it was done for the original winding and is given in figure 10.

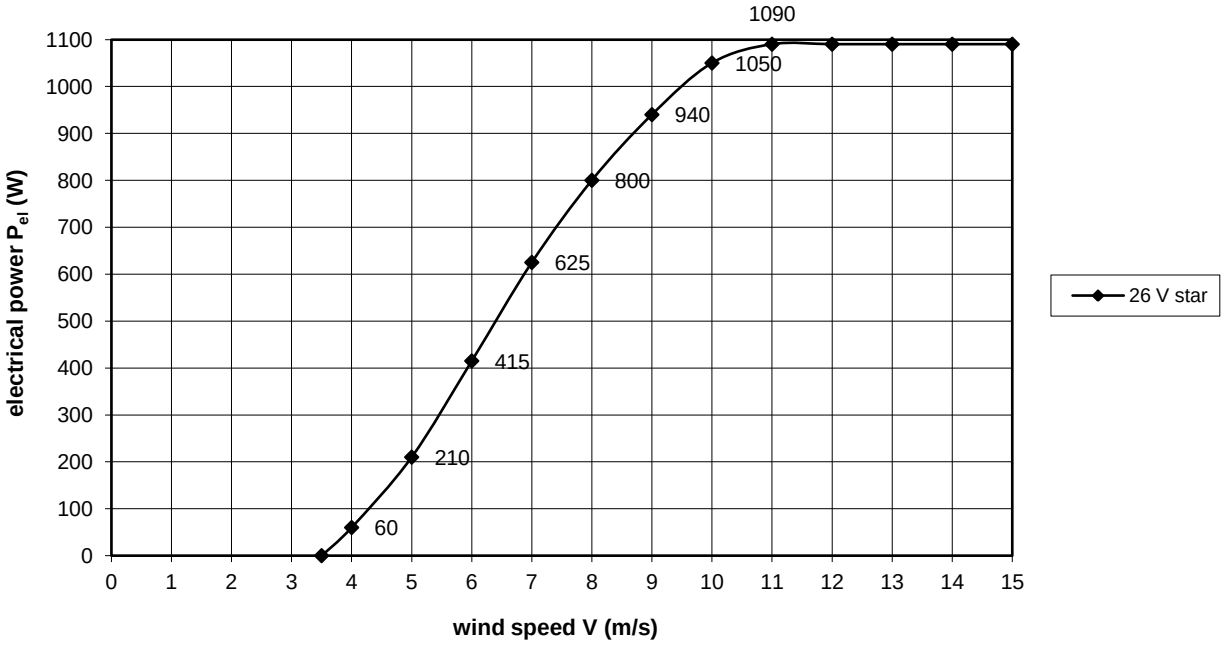

fig. 10 P_{el}-V curve of the VIRYA-3.9 windmill for 26 V star for the modified 115/200 V winding

If figure 10 is compared to the curve for 26 V delta in figure 7, it can be seen that the cut-in wind speed is increased from 3.3 m/s up to 3.5 m/s. However, the maximum electrical power is increased from 910 W up to 1090 W. So a battery charge controller which can dissipate a maximum power of 1200 W is certainly large enough.

If figure 10 is compared to the curve for 26 V star in figure 7, it can be seen that the cut-in wind speed is increased from 2.4 m/s up to 3.5 m/s. However, the maximum electrical power is increased from 670 W up to 1090 W.

So the much higher electrical power for the modified winding for 26 V star results in less heat dissipation in the winding and so in a lower generator temperature at high power.

It will be clear that it is also possible to use the original 230/400 V winding rectified in star for 48 V battery charging and that then the same P_{el}-V curve is valid as given in figure 10.

8 Alternative 3-bladed VIRYA-3.9B3 rotor

The disadvantage of a 2-bladed rotor is that the gyroscopic moment in the rotor shaft is fluctuating. It is maximal for the blades in the vertical position and zero for the blades in the horizontal position. This fluctuation can be flattened by using an elastic element which connects both blades. The connecting strip of the 2-bladed VIRYA-3.9 is rather flexible but as the blades are rather heavy, it isn't sure if the fluctuation of the gyroscopic moment is flattened enough. Fluctuation of the gyroscopic moment results in vibration of the tower if the frequency of the fluctuation is the same as the natural frequency of the tower.

The gyroscopic moment in one blade is always fluctuating but the resulting moment of three blades on the rotor shaft is constant for a constant rotational speed of the rotor and a constant angular velocity of the head. So a 3-bladed rotor isn't giving vibration of the tower. It is possible to design a 3-bladed rotor with the same design tip speed ratio $\lambda_d = 6$ as used for the 2-bladed VIRYA-3.9. The windmill with this rotor is called the VIRYA-3.9B3.

As the product of the number of blades B and the chord c must have a certain value for a certain lift coefficient, a certain design tip speed ratio and a certain rotor radius r, the chord of this 3-bladed rotor must be 2/3 of that of the 2-bladed rotor. The same stainless steel sheet size 1500 * 3000 * 3 mm is used. First this sheet is cut into nine sheets size 333 * 1500 mm. As 9 * 333 = 2997 mm, 3 mm is left and so this 3 mm must be cut from the last strip to make that all nine sheets have the same weight!

Two tapered blades are ground form one sheet after cambering. It is assumed that 3 mm is needed for the rectangular grinder. So the effective width is 333 – 3 = 330 mm. The blade width b at the tip is 180 mm for the 2-bladed rotor. So it is assumed that it is 120 mm for the 3-bladed rotor. So the strip width at the blade root is 330 – 120 = 210 mm. So the width increases from the blade tip to the blade root by 210 – 120 = 90 mm. The blade is calculated for six stations which have a distance of 300 mm with respect to each other so the width increases by 90 / 5 = 18 mm per station. The camber radius r_c should also be about 2/3 of the camber radius of the 2-bladed rotor. It is chosen that $r_c = 230$ mm. The cord c and the camber C are calculated in the same way as it was done for the 2-bladed rotor and the result is given in table 4.

Station	b (mm)	r_c (mm)	α_c (rad)	c (mm)	c (m)	C (%)
A	120	230	0.2609	118.7	0.1187	6.56
B	138	230	0.3000	135.9	0.1359	7.56
C	156	230	0.3391	153.0	0.153	8.56
D	174	230	0.3783	169.9	0.1699	9.57
E	192	230	0.4174	186.5	0.1865	10.59
F	210	230	0.4565	202.8	0.2028	11.61

table 4 Calculated values of the chord c and the camber C for different stations

This rotor has three 0.75 m long spokes made out of stainless steel strip size 80 * 10 mm which make an angle of 120° with each other. The three strips are welded together at the centre and clamped in between the hub and a clamping disk by means of three bolts M12. The rotor calculations are similar as for the 2-bladed rotor. Formula 1, 2, 3 and 5 are still valid. Substitution of B = 3 in formula (5.4) of KD 35 gives:

$$C_l = 8.378 * r (1 - \cos\phi) / c \qquad (-) \qquad (11)$$

The Reynolds values for the stations are calculated for a wind speed of 5 m/s. Those airfoil Reynolds numbers are used which are lying closest to the calculated values. The result of the calculations is given in table 5.

station	r (m)	λ_{rd} (-)	ϕ (°)	c (m)	$C_{l\,th}$ (-)	$R_{e\,r} * 10^{-5}$ V = 5 m/s	Camber C (%)	Camber used (%)	$R_e * 10^{-5}$	α_{th} (°)	β_{th} (°)	β_{real} (°)
A	1.95	6	6.3	0.1187	0.83	2.39	6.56	7.14	2.5	0.8	5.5	3.5
B	1.65	5.077	7.4	0.1359	0.85	2.32	7.56	7.14	2.5	0.9	6.5	5.8
C	1.35	4.154	9.0	0.153	0.91	2.15	8.56	7.14 + 10	2.5	0.9	8.1	8.1
D	1.05	3.231	11.5	0.1699	1.03	1.87	9.57	10	1.7	1.9	9.6	10.4
E	0.75	2.308	15.6	0.1865	1.24	1.49	10.59	10	1.7	3.3	12.3	12.7
F	0.45	1.385	23.9	0.2028	1.59	1.04	11.61	12.5	1.2	7.9	16.0	15.0

table 5 Calculation of the blade geometry of the VIRYA-3.9B3 rotor

In table 5 it can be seen that the theoretical lift coefficient C_{lth} is not constant but increasing at decreasing values of r. But the increase is less than for a constant chord blade.

The camber is increasing from 6.56 % at station A the to 11.61 % at station F. To find the theoretical angles of attack α_{th}, we need C_l-α curves for the six different cambers. However, only characteristics for 7.14 %, 10 % and 12.5 % are available in KD 398. The C_l-α curve for 7.14 % camber was used for station A and B. The average angle of the C_l-α curves for 7.14 % and 10 % camber was used for station C. The C_l-α curve for 10 % camber was used for stations D and E. The C_l-α curve for 12.5 % camber was used for station F.

In table 5 it can be seen that the theoretical blade angles β_{th} vary in between 5.5° at the blade tip and 16.0° at station F. In the table at figure 1 of report KD 616 it can be seen that the blade angle at the blade tip is only 2.1°, so much smaller than 5.5°. A problem with a rotor made out of a cylinder is that only the blade angle at the blade tip β_A can be adjusted at a certain value. The blade angles at other stations depend on the taper of the blade and are difficult to calculate for a certain value of β_A. They are given on the composite drawing of the cross sections of the 1.8 m rotor which is given at the right side in figure 1 of KD 616. A similar composite drawing was made for the six stations of a VIRYA-3.9B3 blade for different values of β_A. The composite drawing for the right blade seen from the right side is given as figure 11. It was found that β_A = 3.5° gives real values of β for the sections B, C, D, E and F which are matching best with the calculated values of β_{th} in table 5. A drawing of the whole rotor is given in figure 12. The distance in between the heart of a spoke and the tailing edge of the blade is chosen 95 mm (in a flat plane). The spoke has to be twisted 12.5° right hand in between the hub and the blade root. A spoke has to be bevelled over the outer 300 mm at the left and right backside by an angle of 6° to prevent flattening of the blade when the bolts are tightened. A blade is connected to a spoke by three bolts M12 * 45. The bolt head is at the backside. A heavy washer has to be mounted under the head of the outer bolt to prevent a too high stress in the blade at this point because of the rotor thrust.

The mass of one blade is about 5.79 kg. The mass of one spoke is about 4.56 kg. The mass of the hub is about 1.95 kg. The mass of the clamping disk is about 0.39 kg. So the mass of the whole rotor is about 33.4 kg. This is acceptable for a stainless steel 3-bladed rotor with a diameter of 3.9 m.

It might be possible to use this rotor to drive a centrifugal pump through a vertical shaft in the centre of the tower and an accelerating transmission in the head but description of this option is out of the scope of this report.

The maximum C_p of a 3-bladed rotor is somewhat higher than for a 2-bladed rotor with the same design tip speed ratio because the tip losses for a 3-bladed rotor are less than for a 2-bladed rotor (see KD 35 figure 4.3). However, the Reynolds values of the 3-bladed rotor are lower resulting in a higher C_d/C_l ratio and this results in a lower maximum C_p. It is assumed that both effects compensate each other and so it is assumed that the C_p-λ and C_q-λ curves as given in chapter 4 for the VIRYA-3.9 are also valid for the VIRYA-3.9B3. So the P-n curves and the P_{el}-V curves as given in chapter 5 and chapter 7 are also valid for the VIRYA-3.9B3. The starting behaviour as explained in chapter 6, will also be the same.

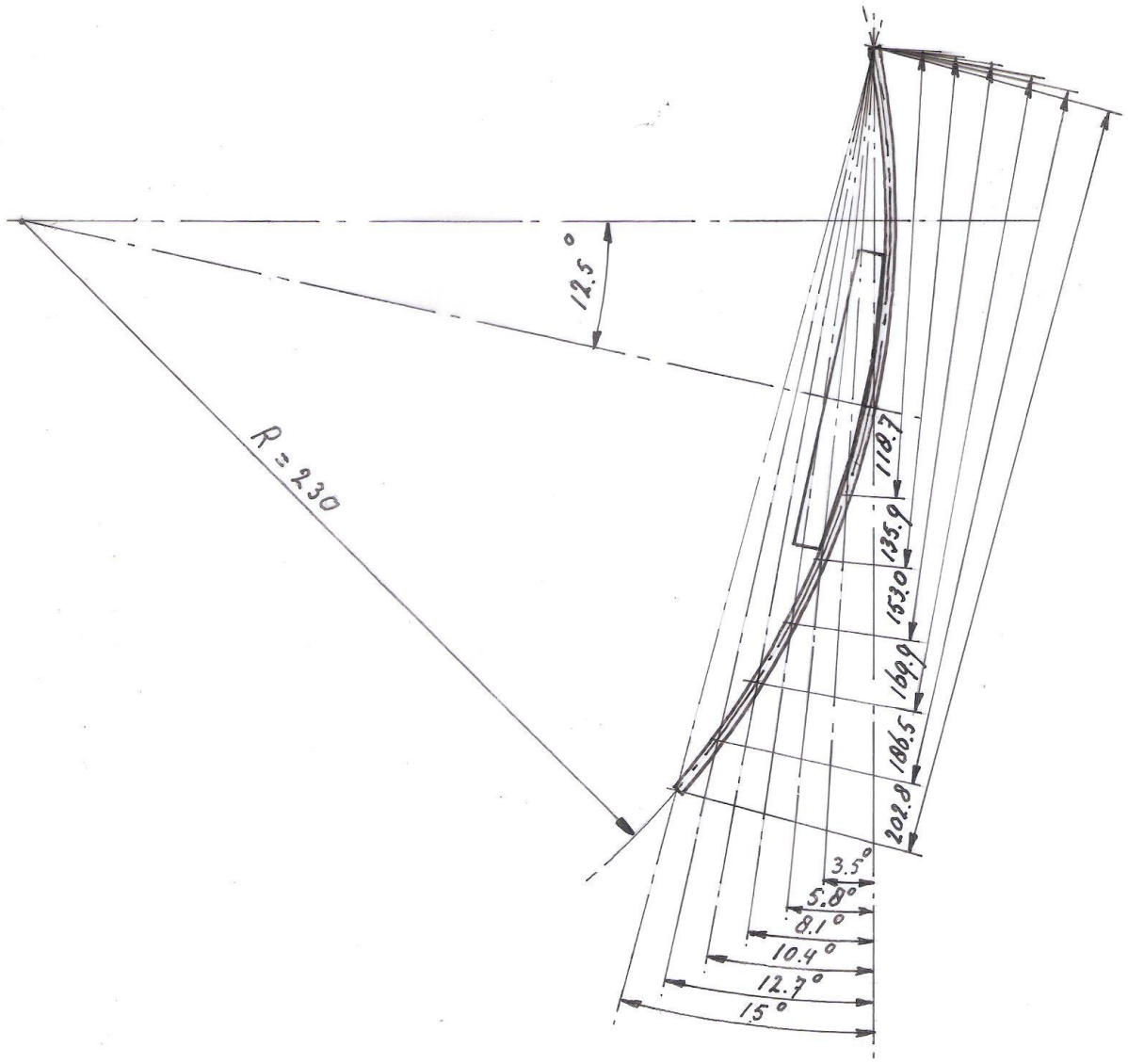

fig. 11 The right blade for six stations A, B, C, D, E and F

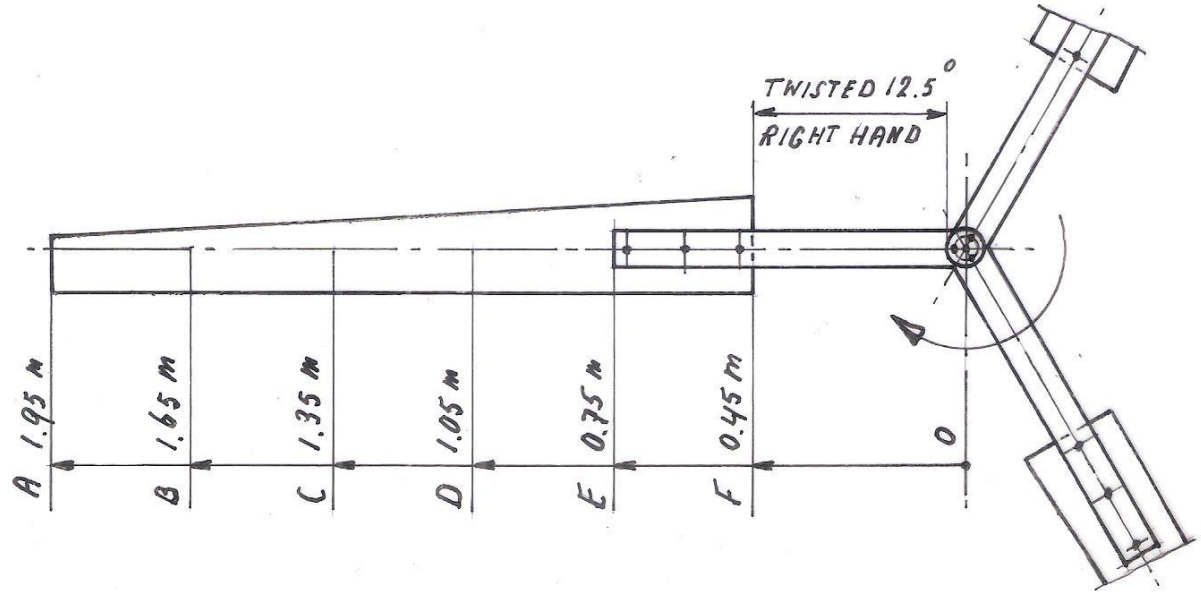

fig. 12 Front view of the VIRYA-3.9B3 rotor

9 Use of a PM-generator of Hefei Top Grand type TGET380-10KW-1200R

Instead of the VIRYA-4.2 generator, it might be possible to use a Chinese PM-generator of Hefei Top Grand type TGET380-10KW-1200R. For checking of the matching in between rotor and generator and for the determination of the P_{el}-V curve, measured P_{mech}-n and P_{el}-n curves of the generator for a 24 V battery load are needed. A 24 V battery is charged at an average charging voltage of about 26 V so the P_{mech}-n curve and the P_{el}-n curve should have been measured for this constant voltage. However, Hefei Top Grand supplies only a P_{el}-n curve for a resistance load. The resistance R is chosen that high that the electrical power is 10 kW = 10000 W at a rotational speed of 1200 rpm and a loaded alternating voltage of 220 VAC. But the characteristics for a resistance load differ very much from the characteristics for a constant voltage. So the characteristics for a constant voltage of 26 V have to be estimated to check the matching in between rotor and generator (see chapter 10).

My PM-generator using a motor housing 5RN90L04V has been measured for different load conditions. The measurements are given in report KD 78 (ref. 10). The measurements for a constant resistance are given at chapter 7 and 9 of KD 78. The unloaded U-n curve is a straight line through the origin (see KD 78 figure 1) but it can be derived that the U-n curve and the Q-n curve for a resistance load are also about straight lines through the origin. Figure 31 and figure 32 of KD 78 show that the P_{mech}-n and P_{el}-n curves are about parabolas if the torque is not close to the maximum torque level which the generator can supply. This is in accordance with the U_{AC}-n and P_{el}-n curves given at point 6 of the data sheet of Hefei Top Grand. These curves give measuring points every 100 rpm but the values of the measuring points are not given. So these curves are estimated from the given values at n =1200 rpm.

The winding is a 3-phase winding connected in star. The star point is lying internal so only the three phase wires are coming through the hollow generator shaft. The given voltage is the alternating voltage U_{AC} in between two of the three phases. For battery charging, the winding must be rectified. The rectified DC voltage U_{DC} is a factor 0.955 * $\sqrt{2}$ = 1.3506 higher than U_{AC} (if the voltage drop of the rectifier diodes is neglected). The unloaded or open voltage U_{open} is also not specified. For a smaller generator type TGET320-1KW-350R, it has been found in chapter 3 of report KD 705 (ref. 11) that the ratio U_{open} / U_{DC} is about 68 / 56 = 1.2143. It is assumed that this ratio is also valid for the generator type TGET380-10KW-1200R. So for the loaded DC voltage U_{DC} at n = 1200 rpm it is valid that U_{DC} = 1.3506 * 220 = 297 VDC. For the open DC voltage U_{open} at n = 1200 rpm it is valid that U_{open} = 1.2143 * 0.955 * $\sqrt{2}$ * 220 = 361 VCD. The calculated values are given in the bottom line of table 6.

n (rpm)	U_{AC} (V)	U_{DC} (V)	U_{open} (V)	P_{el} (W)	η_{gen} (-)	P_{mech} (W)	Q (Nm)	P_{heat} (W)
0	0	0	0	0	-	0	0	0
100	18.3	24.8	30.1	69.4	0.85	81.7	7.8	5.3
200	36.7	49.5	60.2	277.8	0.85	326.8	15.6	49.0
300	55	74.3	90.3	625	0.85	735.3	23.4	110.3
400	73.3	99.0	120.3	1111.1	0.85	1307.2	31.2	196.1
500	91.7	123.8	150.4	1736.1	0.85	2042.5	39.0	306.4
600	110	148.5	180.5	2500	0.85	2941.3	46.8	441.3
700	128.3	173.3	210.6	3402.8	0.85	4003.4	54.6	600.6
800	146.7	198.0	240.7	4444.4	0.85	5228.9	62.4	784.4
900	165	222.8	270.8	5625.0	0.85	6617.8	70.2	992.8
1000	183.3	247.5	300.8	6944.4	0.85	8170.1	78.0	1225.7
1100	201.7	272.3	330.9	8402.8	0.85	9885.9	85.8	1483.1
1200	220	297	361	10000	0.85	11765	93.6	1765

table 6 U_{AC}, U_{DC}, U_{open}, P_{el}, η_{gen}, P_{mech}, Q and P_{heat} as a function of n

No rated torque Q is given for the generator. However, it is specified at point 5 of the data sheet that the generator efficiency η_{gen} is at least 85 %. In figure 33 of KD 78 (ref. 7) it can be seen that the efficiency for a resistance load is about constant for every rotational speed and that it is high if the load resistance isn't low. It is easy to give the efficiency as a factor of 1 and it is assumed that $\eta_{gen} = 0.85$ for all rotational speeds. As the generator has no iron in the coils, the heat losses P_{heat} are only caused by the copper losses in the winding. The P_{mech}-n, the P_{heat}-n and the Q-n curves of the generator can be derived by the formulas:

$$P_{mech} = P_{el} / \eta_{gen} \quad (W) \qquad (12)$$

$$P_{heat} = P_{mech} - P_{el} \quad (W) \qquad (13)$$

$$Q = 30\, P_{mech} / (\pi * n) \quad (Nm) \qquad (14)$$

First the values of P_{mech}, P_{heat} and Q are determined for n = 1200 rpm. Substitution of $P_{el} = 10000$ W and $\eta_{gen} = 0.85$ in formula 12 gives that $P_{mech} = 11765$ W. Substitution of $P_{mech} = 11765$ and $P_{el} = 10000$ W in formula 13 gives that the heat loss $P_{heat} = 1765$ W. Substitution of $P_{mech} = 11765$ W and n = 1200 rpm in formula 14 gives that Q = 93.6 Nm. These values are also given in the bottom line of table 6.

The values for other rotational speeds are now calculated assuming that the U-n and Q-n curves are straight lines through the origin and that the P-n curves are parabolas. The wanted curves can now be derived from table 6. The U_{AC}-n, the U_{DC}-n and the U_{open}-n curves are given in figure 13.

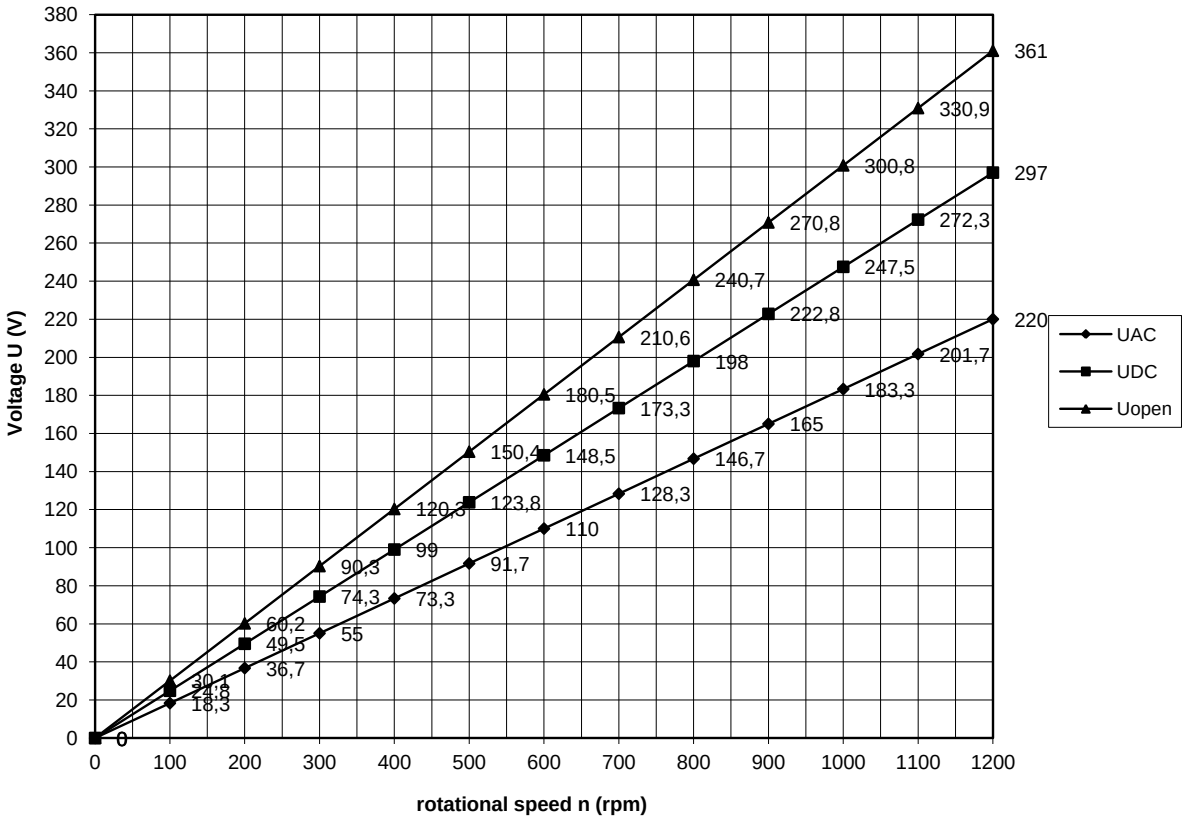

fig. 13 U_{AC}, U_{DC} and U_{open} as a function of n for a resistance load

The P_{mech}-n and the P_{el}-n curves are given in figure 14.

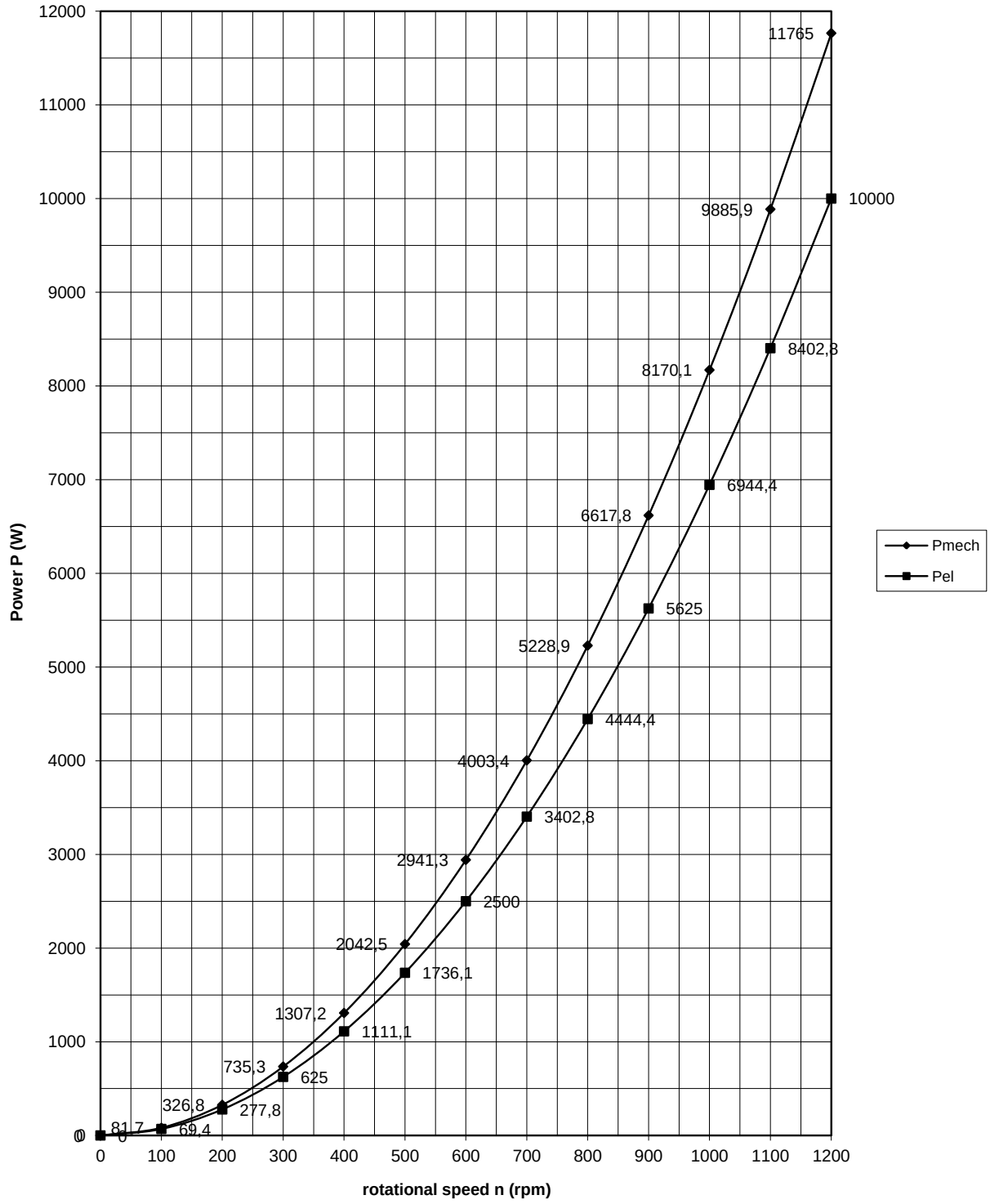

fig. 14 P_{mech} and P_{el} as a function of n for a resistance load

The Q-n curve is given in figure 15.

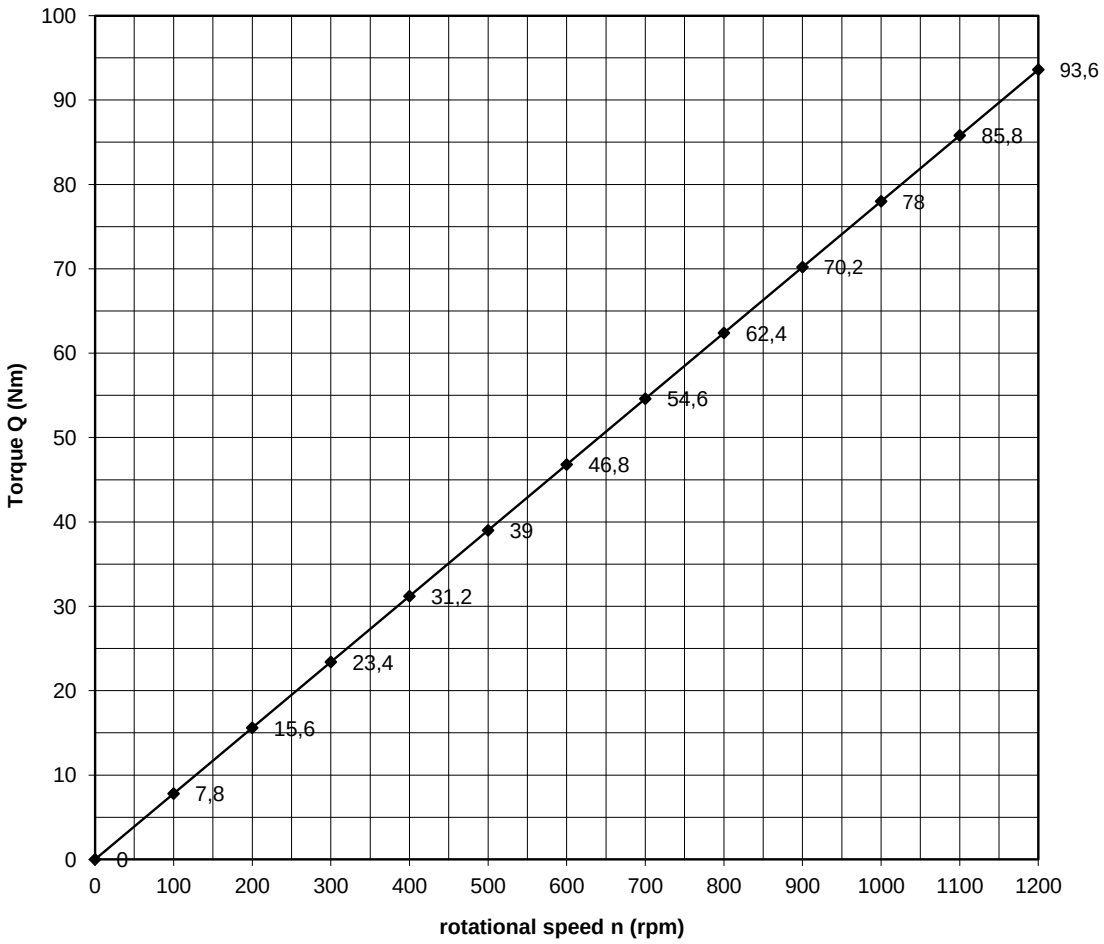

fig. 15 Loaded torque Q as a function of n for a resistance load

So figure 13, 14 and 15 are based on the manufactures specification for a resistance load at n = 1200 rpm. The load resistance R can be calculated if it is assumed that three identical resistors are connected in star to the three phase wires. The voltage over one resistor is equal to the phase voltage U_f = 127.02 V. The current I = 26.24 A at n = 1200 rpm. So according to the law of Ohm, the resistance R is given by R = U / I or R = 127.02 / 26.24 = 4.84 Ω.

If three resistors are used as load, the winding of one phase is used for all the time to generate power. This power varies according to a $\sin^2 \alpha$ function. The power fluctuation is given in figure 2 of report KD 340 (ref. 12). If a 3-phase winding is rectified in star, only two of the three phases are generating power at the same time. This means that in one phase, power is only generated for $30° < \alpha < 150°$ and for $210 < \alpha < 330°$. This means that no power is generated for $0° < \alpha < 30°$, for $150° < \alpha < 210°$ and for $330° < \alpha < 360°$. The loss of generated power because of this effect is about 7 % of the power generated for a resistance load. But this effect is neglected and so it is assumed that the generator is able to generate a DC power of 10 kW at n = 1200 rpm.

10 Determination of the P_{mech}-n and the P_{el}-n curves for 26 V star

If this generator is used for 24 V battery charging, it is used at much lower rotational speeds than the nominal rotational speed of 1200 rpm. It is assumed that the average charging voltage for a 24 V lead acid battery is 26 VDC. So P_{mech}-n and P_{el}-n curves for 26 V star are needed to check the matching in between rotor and generator and to derive the P_{el}-V curve. The best way is to buy a generator and to test it on a large accurate test rig. I have used the test rig of the University of Technology Eindhoven to test the original VIRYA-4.2 generator. But obtaining the generator and hiring of the test rig is expensive and I won't do that. So it is tried to estimate the wanted characteristics from the curves as given in chapter 3.

The PM-generator which is used for the measurements as given in KD 78 (ref. 10) was measured for different constant voltages rectified in star. The Q-n curves for 26 V star, 52 V star and 76 V star are given in figure 8 of chapter 4 of KD 78. The Q-n curve for short-circuit in star before the rectifier is given in figure 4 of chapter 3 of KD 78. If these curves are compared it can be seen that all curves have about the same shape but that the curve is shifted to the right if the voltage is higher. All curves have about the same maximum value of about 29 Nm. The first part of each curve, up to about 2/3 of the peak value, so up to a torque of about 20 Nm, is about a straight line but the curves bend to the right for higher torques. The curves start at the rotational speed for which the open generator voltage is equal to the average charging voltage. The phenomenon is used to derive the wanted characteristics of the generator type TGET380-10KW-1200R for 26 V star.

In figure 15 it can be seen that the nominal torque Q at 1200 rpm is 93.6 Nm. In figure 13 it can be seen that the loaded DC voltage U_{DC} is 297 VDC at n = 1200 rpm. So first the Q-n curve is determined for a constant voltage of 297 VDC. A horizontal line is drawn in figure 13 for U = 297 VDC until it intersects with the U_{open}-n curve. The point of intersection lies about at a rotational speed of 990 rpm. It is assumed that the sticking torque of the generator can be neglected and so the unloaded torque is zero at n = 990 rpm. It is also assumed that the nominal torque Q = 93.6 Nm is lying that far from the peak torque that it is allowed to assume that the Q-n curve for a constant voltage of 297 VDC is a straight line. Figure 15 is now copied as figure 16 and the Q-n curve for 297 VDC is added. So the Q-n curve for 297 VDC is a straight line going through the point Q = 0 Nm and n = 990 rpm and the point Q = 93.6 Nm and n = 1200 rpm. This curve is also drawn in figure 16. The difference in between the rotational speeds is 1200 – 990 = 210 rpm.

Next the Q-n curve for 26 VDC is determined by shifting the Q-n curve for 297 VDC to the left. It must be shifted that far, that is starts at the rotational speed belonging to an open voltage of 26 VDC. In figure 13 it can be seen that an open voltage of 26 VDC is reached at a rotational speed of about 87 rpm. To get a Q-n curve for 26 VDC which is in parallel to the Q-n curve for 297 VDC, the maximum torque of 93.6 Nm must lie at a rotational speed of 87 + 210 = 297 rpm. So the Q-n curve for 26 VDC is a straight line going through the point Q = 0 Nm and n = 87 rpm and the point Q = 93.6 Nm and n = 297 rpm. This curve is also drawn in figure 16.

Next the Q-n curve for short-circuit in star is determined by shifting the Q-n curve for 297 VDC that far to the left that it starts at the origin of the graph. So the Q-n curve for short-circuit in star is a straight line going through the point Q = 0 Nm and n = 0 rpm and the point Q = 93.6 Nm and n = 210 rpm. This curve is also drawn in figure 16.

It will be clear that the efficiency for short-circuit in star is zero as all generated power is dissipated as heat in the winding. The efficiency for 26 V star is only 0.85 for the point of intersection of the Q-n curve for a resistance load and the Q-n curve for 26 VDC. This point of intersection lies about at a rotational speed of 107 rpm. The efficiency may have a maximum of about 0.9 for a rotational speed of about 97 rpm. The efficiency for rotational speeds higher than 107 rpm will be lower than 0.85 and it is assumed that it is 0.53 for n = 297 rpm.

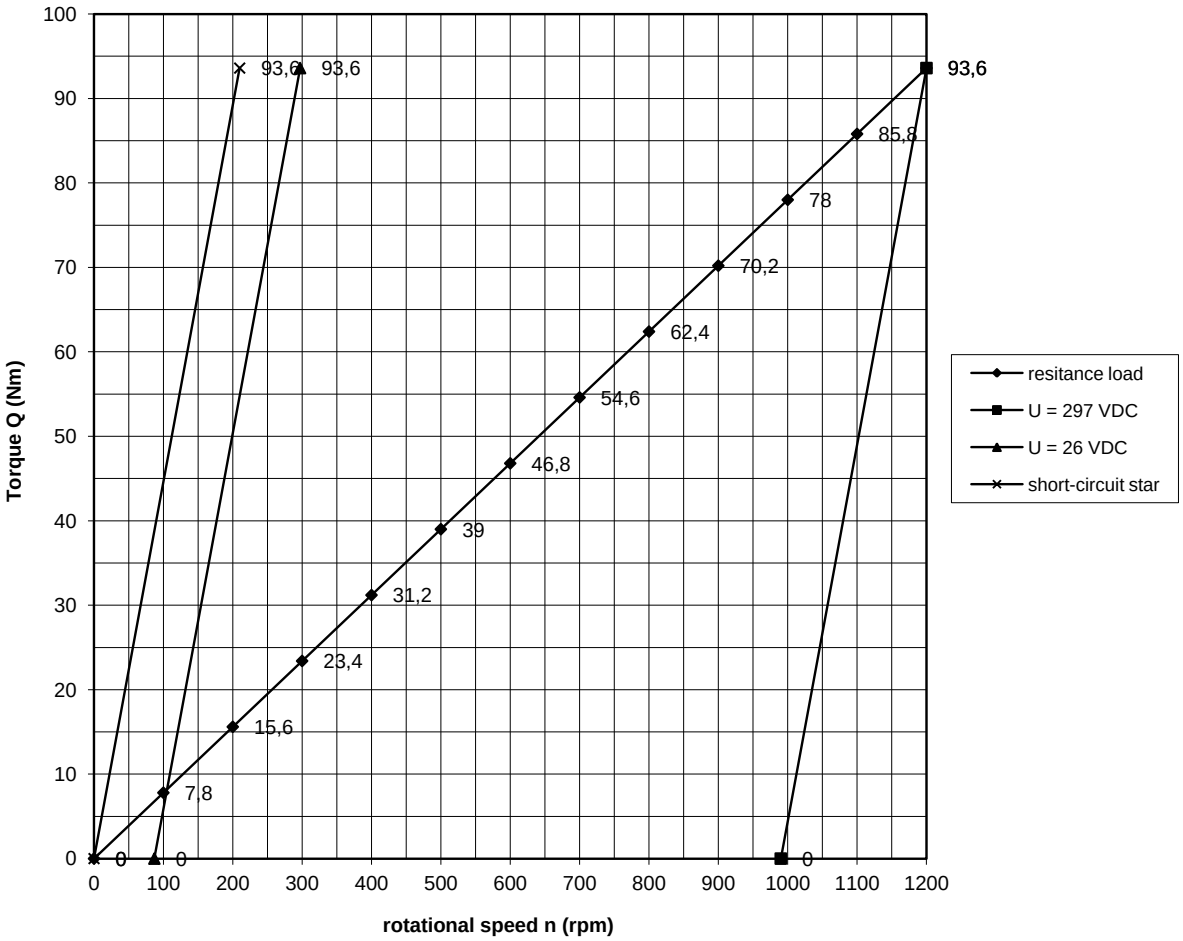

fig. 16 Q-n curve for a resistance load, for constant voltages of 297 VDC and for 26 VDC and for short-circuit in star

For the determination of the P_{mech}-n and the P_{el}-n curves it is necessary to take several points on the Q-n curves. The curves for 26 V star are determined first. The values of Q are determined for rotational speeds of 87 rpm up to 297 rpm in steps of 10 rpm. The results are given in table 7. P_{mech} and P_{el} are calculated with:

$$P_{mech} = Q * n * \pi / 30 \qquad (W) \qquad (15)$$

$$P_{el} = \eta_{gen} * P_{mech} \qquad (W) \qquad (16)$$

So for the determination of P_{el}, it is necessary to estimate a η_{gen}-n curve. The estimated η_{gen}-n curve is given in figure 17. It is assumed that the efficiency curve has a peak $\eta_{gen} = 0.9$ for n = 97 rpm and that $\eta_{gen} = 0.85$ for n = 107 rpm.

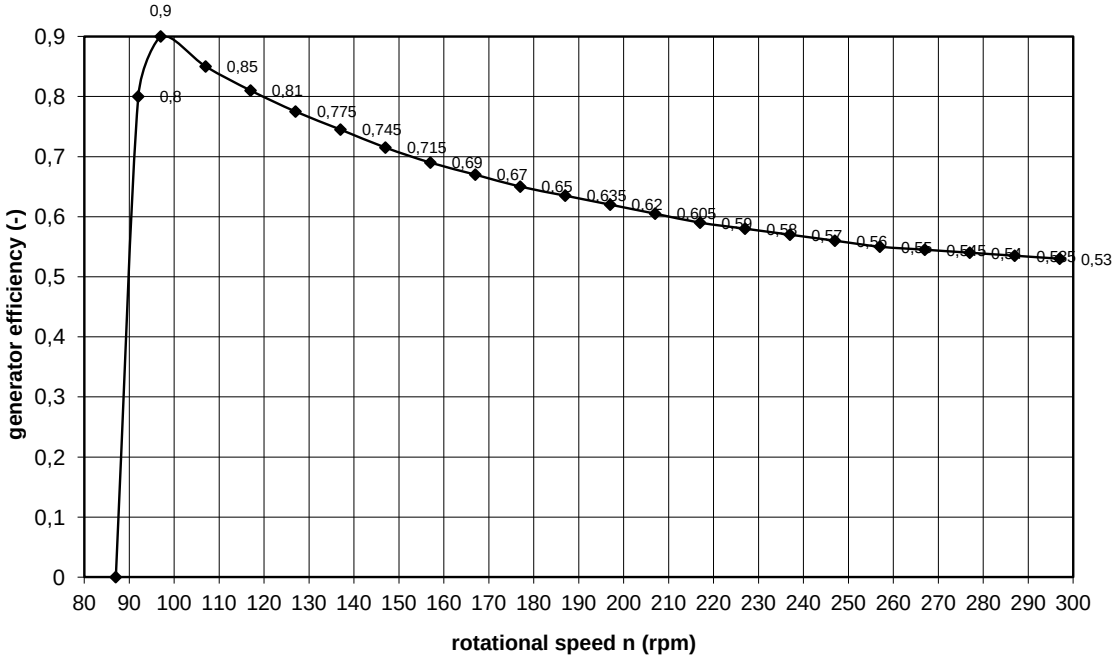

fig. 17 Estimated η_{gen}-n curve for 26 V star for generator TGET380-10KW-1200R

n (rpm)	Q (Nm)	P_{mech} (W)	η_{gen} (-)	P_{el} W	P_{heat} (W)
87	0	0	0	0	0
92	2.23	21.5	0.8	17.2	4.3
97	4.46	45.3	0.9	40.8	4.5
107	8.91	99.8	0.85	84.9	14.9
117	13.37	163.8	0.81	132.7	31.1
127	17.83	237.1	0.775	183.8	53.3
137	22.29	319.8	0.745	238.2	81.6
147	26.74	411.6	0.715	294.3	117.3
157	31.20	513.0	0.69	353.9	159.1
167	35.66	623.6	0.67	417.8	205.8
177	40.11	743.5	0.65	483.2	260.3
187	44.57	872.8	0.635	554.2	318.6
197	49.03	1011.5	0.62	627.1	384.4
207	53.49	1159.5	0.605	701.5	458.0
217	57.94	1316.6	0.59	776.8	539.8
227	62.40	1483.3	0.58	860.3	623.0
237	66.86	1659.4	0.57	945.8	713.6
247	71.31	1844.5	0.56	1032.9	811.6
257	75.77	2039.2	0.55	1121.6	917.6
267	80.23	2243.2	0.545	1222.6	1020.6
277	84.69	2456.6	0.54	1326.6	1130.0
287	89.14	2679.1	0.535	1433.3	1245.8
297	93.6	2911.1	0.53	1542.9	1368.2

table 7 Calculated values of Q, P_{mech}, η_{gen}, P_{el} and P_{heat} as a function of n for 26 V star

Figure 9 is now copied as figure 17 and the characteristics of the original VIRYA-4.2 generator are removed. The new P_{mech}-n and P_{el}-n curves for the generator type TGET380-10KW-1200R can be derived from table 7 and are given in figure 18.

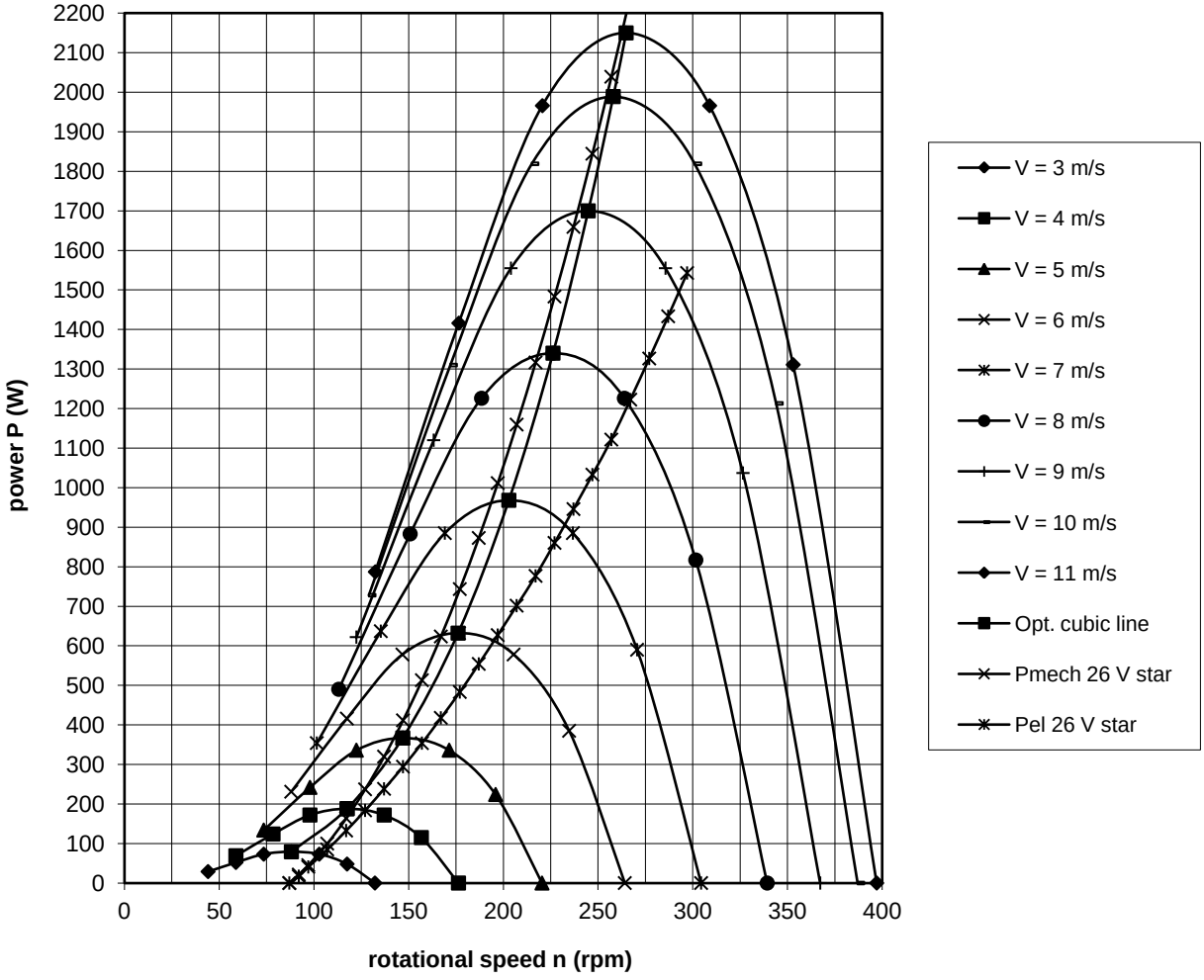

fig. 18 P-n curves and optimum cubic line of the VIRYA-3.9 rotor, estimated P_{mech}-n and P_{el}-n curves for 26 V star for generator type TGET380-10KW-1200R

In figure 18 it can be seen that the matching is very good because the P_{mech}-n curve of the generator for 26 V star is lying close to the optimum cubic line of the rotor.

The point of intersection of the P_{mech}-n curve of the generator with the P-n curve of the rotor for a certain wind speed is the working point for that wind speed. The electrical power for that wind speed is found by going downwards vertical until the P_{el}-n curve is reached. The values of P_{el} found this way is given in the P_{el}-V curve of figure 19.

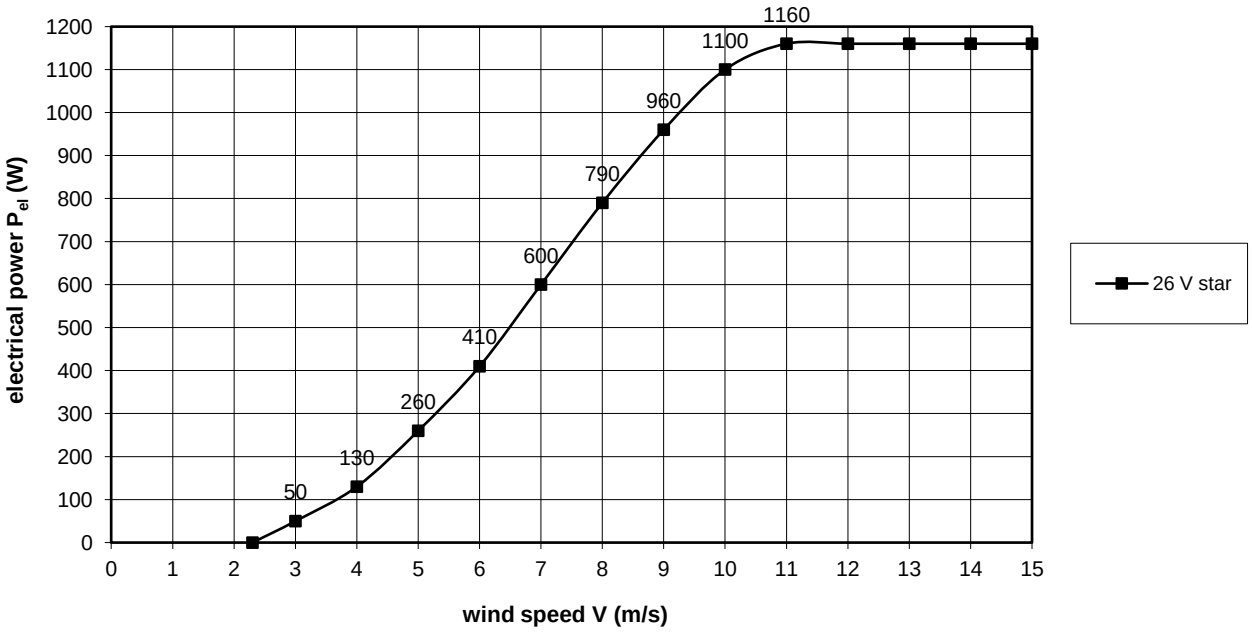

fig. 19 Estimated P_{el}-V curve for 26 V star

The P_{el}-V curve starts at a wind speed of about 2.3 m/s so the $V_{cut\ in}$ = 2.3 m/s. This means that the VIRYA-3.9 can be used in regions with rather low wind speeds.

In chapter 4 it has been calculated that the starting wind speed V_{start} = 2.9 m/s if the sticking torque of the original generator is 0.9 Nm. For the new generator of Hefei Top Grand it is specified that the sticking torque is smaller than 0.3 Nm. However, this is the case if no shaft seal is used. A shaft seal is needed with horizontal positioning of the shaft and this seal will cause a rather large sticking torque especially if it is new. So it can be expected that the starting wind speed is about 3.5 m/s This means that there is hysteresis in the P_{el}-V curve for $2.3 < V < 3.5$ m/s.

The maximum electrical power is about 1160 W. This is 60 W higher than for the original VIRYA-4.2. The mechanical power at V = 11 m/s is about 2140 W at n = 270 rpm. The corresponding electrical power is about 1160 W. So this gives for the heat losses that P_{heat} = 2140 – 1160 = 980 W. If the generator is used with a resistance load at n = 1200 rpm, the electrical power is 10000 W. If the efficiency is 0.85, it means that the mechanical power is 10000 / 0.85 = 11765 W and so the heat losses are 1765 W. So although the efficiency at 26 VDC and a maximum rotational speed of about 270 rpm is rather low (about 0.55), the generated heat is certainly acceptable. So the generator type TGET380-10KW-1200R can be used in combination with the VIRYA-3.9 rotor for 24 V battery charging.

The P_{mech}-n, the P_{el}-n curves as given in figure 18 and the P_{el}-V as given in figure 19 are estimated and not measured like it was done for the original generator. Measured characteristics are more accurate than estimated characteristics. So to be sure that an acceptable matching is realised for the generator of Hefei Top Grand, it is necessary to buy one and to test it at a large test rig with which it is possible to also measure the torque Q.

If such a test rig isn't available, at least one has to measure the open DC voltage as a function of the rotational speed and check if the real U_{open}-n curve is about the same as the estimated U_{open}-n curve as given in figure 13. It is also advised to connect the generator to a large almost empty 24 V lead acid battery and check if the measured P_{el}-n curve is about the same as the estimated P_{el}-n curve given in figure 18. If this is the case, one may assume that the P_{mech}-n curve is also almost the same and so the matching will be acceptable.

The axial flux generator type TGET380-10KW-1200R has a collar at the front side with a diameter of 140 mm and ten threaded holes M12 at a pitch circle of 120 mm. This hole pattern doesn't match with the spoke assembly of the 3-bladed VIRYA-3.9B3.

So it is expected that only the 2-bladed VIRYA-3.9 is used in combination with this generator. The two blades of the VIRYA-3.9 are originally connected to each other by a strip size 10 * 100 * 1500 mm. So the strip width is smaller than the pitch circle of the threaded holes. Therefore it is better to use strip size 8 * 150 *1500 mm if this axial flux generator is used. This strip has to be cambered with the same radius as used for the blades for the 300 mm long outer parts where it overlaps a blade. It seems good to add two extra bolts M10 at the corners of the strip to prevent stress concentration in the sheet at the outer bolt M12.

It is specified by the manufacturer that the depth of the thread M12 in the collar is 20 mm which seems rather small. It should be checked if it is possible to use ten bolts M12 * 35. One has to use locking washers and locking liquid at these bolts!

For 24 V battery charging one needs a voltage controller plus dump load to limit the maximum charging voltage up to 27.6 V to prevent over charging when the battery is full. A 27.6 V, 200 W controller is described in a free public manual which is available at my website at the bottom of the menu KD-reports (ref. 13). As the VIRYA-3.9 can produce a maximum power of about 1160 W, at least six, 200 W dump loads have to be connected in parallel. Only one voltage controller is needed. Two identical 12 V lead acid batteries of at least 200 Ah have to be connected in series.

Building of the VIRYA-3.9 with this generator type TGET380-10KW-1200R is only possible if the drawings of the rotor, the head and the tower are available. Figure 1 gives an impression of the rotor but detailed drawings have to be made. A drawing of an hydraulic blade press to camber the blades must also be made. From 1-1-2018 Kragten Design is no longer a commercial company and licences and drawings of the bigger VIRYA windmills are no longer supplied. The final drawings of the VIRYA-3.9 have to be made by the company which is interested to build this VIRYA-3.9 wind turbine in series. If a company is interested, I can make photos of the original drawings of the head and the tower of the VIRYA-4.2. Both drawings are made on paper sheet size A1 and therefore too big to add to this report.

It seems also possible to use the VIRYA-3.9 for grid connection. However, then it is better to chose an axial flux PM-generator with a higher nominal voltage at a lower rotational speed. Assume the generator type TGET380-5KW-500R is chosen. This generator generates 5000 W at 500 rpm and it has a loaded voltage of 415 VAC at 500 rpm. If the efficiency is 0.85, the mechanical power P_{mech} = 5882 W at 500 rpm. Substitution of P_{mech} = 5882 W and n = 500 rpm in formula 14, gives that Q = 112.3 Nm. This is higher than Q = 93.6 Nm at n = 1200 rpm of the TGET380-10KW-1200R and so the generator TGET380-5KW-500R is certainly strong enough for grid connection.

Instead of the 12 m high 3-legs VIRYA-4.2 tower, it seems also possible to use the 8.6 m high tubular tower which is described in report KD 582 (ref. 14).

11 References

1 Kragten A. Verslag van windtunnelmetingen aan 2 bladige rotoren met uit een cylinder gemaakte bladen (in Dutch), June 1978, report R 343 D, former Wind Energy Group, Laboratory of Fluid Mechanics, Department of Physics, University of Technology Eindhoven, no longer available.

2 Kragten A. Translation of parts of report R 343 D of June 1978 from Dutch into English. R 343 D gives wind tunnel measurements for a rotor with tapered blades made out of a cylinder, November 2016, free public report KD 616, engineering office Kragten Design, Populierenlaan 51, 5492 SG Sint-Oedenrode, The Netherlands.

3 Kragten A. Calculations executed for the 2-bladed rotor of the VIRYA-2.92 windmill (λ_d = 6, stainless steel tapered blades) driving the VIRYA-2.68 PM-generator for 24 V battery charging, June 2018, free public report KD 656, engineering office Kragten Design, Populierenlaan 51, 5492 SG Sint-Oedenrode.

4 Kragten A. Measurements performed on a generator with housing 5RN112M04V and a 4-pole armature equipped with neodymium magnets, June 2004, reviewed September 2016, free public report KD 200, engineering office Kragten Design, Populierenlaan 51, 5492 SG Sint-Oedenrode.

5 Kragten A. Development of the permanent magnet (PM) generators of the VIRYA windmills, May 2007, reviewed December 2017, free public report KD 341, engineering office Kragten Design, Populierenlaan 51, 5492 SG Sint-Oedenrode, The Netherlands.

6 Kragten A. The 7.14 %, 10 % and 12.5 % cambered plate as airfoil for windmill rotor blades, Aerodynamic characteristics, geometry, moment of inertia I and moment of resistance W, November 2008, free public report KD 398, engineering office Kragten Design, Populierenlaan 51, 5492 SG Sint-Oedenrode.

7 Kragten A. Rotor design and matching for horizontal axis wind turbines, January 1999, reviewed February 2017, free public rapport KD 35, engineering office Kragten Design, Populierenlaan 51, 5492 SG Sint-Oedenrode, The Netherlands.

8 Kragten A. Method to check the estimated δ-V curve of the hinged side vane safety system and checking of the δ-V curve of the VIRYA-3.3D windmill (7.14 % cambered steel blades), February 2005, free public report KD 223, engineering office Kragten Design, Populierenlaan 51, 5492 SG Sint-Oedenrode, The Netherlands.

9 Kragten A. Manual of a 27.6 V, 200 W battery charge controller, March 2006, modified December 2016, free public manual available at my website at the bottom of the menu KD-reports, engineering office Kragten Design, Populierenlaan 51, 5492 SG Sint-Oedenrode, The Netherlands.

10 Kragten A. Measurements performed on a generator with housing 5RN90L04V and a 4-pole armature equipped with neodymium magnets, March 2001, reviewed March 2015, free public report KD 78, engineering office Kragten Design, Populierenlaan 51, 5492 SG Sint-Oedenrode, The Netherlands.

11 Kragten A. Ideas about the use of the 3-bladed VIRYA-3B3 rotor (λ_d = 6.5) in combination with the axial flux generator of Hefei Top Grand type TGET320-1KW-350R for 48 V battery charging, August 2020, free public report KD 705, engineering office Kragten Design, Populierenlaan 51, 5492 SG Sint-Oedenrode, The Netherlands.

12 Kragten A. Rectification of 3-phase VIRYA windmill generators, May 2007, reviewed January 2022, free public report KD 340, engineering office Kragten Design, Populierenlaan 51, 5492 SG Sint-Oedenrode, The Netherlands.

13 Kragten A. Manual of a 27.6 V, 200 W battery charge controller, March 2006, modified December 2016, free public manual available at my website at the bottom of the menu KD-reports, engineering office Kragten Design, Populierenlaan 51, 5492 SG Sint-Oedenrode, The Netherlands.

14 Kragten A. Development of a tubular tower for the VIRYA-4.2 and the VIRYA-4.6B2, March 2015, reviewed November 2016, free public report KD 582, engineering office Kragten Design, Populierenlaan 51, 5492 SG Sint-Oedenrode, The Netherlands.